

Decision-dependent Robust Charging Infrastructure Planning for Light-duty Truck Electrification at Industrial Sites: Scheduling and Abandonment

Yifu Ding, Ruicheng Ao, Pablo Duenas-Martinez, Thomas Magnanti

Many industrial sites rely on diesel-powered light-duty trucks to transport workers and small-scale facilities, which has resulted in a significant amount of greenhouse emissions (GHGs). To address this, we developed a two-stage robust charging infrastructure planning model for electrifying light-duty trucks at industrial sites. The model is formulated as a mixed-integer linear programming (MILP) that optimizes the charging infrastructure, selected from multiple charger types and potential locations, and determines opportunity charging schedules for each truck based on the chosen infrastructure. Given the strict stopping points and schedules at industrial sites, we introduced a scheduling-with-abandonment problem, where trucks forgo charging if their waiting times exceed a maximum threshold. We also further incorporated the impacts of overnight charging and range anxiety on drivers' waiting and abandonment behaviors. To represent stochastic, heterogeneous parking durations of trucks, we constructed a decision-dependent robust uncertainty set in which parking time variability flexibly depends on drivers' charging choices. We applied the model in a case study of an open-pit mining site, which plans charger installations in eight zones and schedules a fleet of around 200 trucks. By decomposing the problem into monthly subproblems and using heuristic approaches, for the whole-year dataset, the model achieves an optimality gap of less than 0.1% within a reasonable computation time under diverse uncertainty scenarios.

1. Introduction

1.1. Background

Diesel-powered light-duty trucks are used for transporting and dispatching goods in urban environments and industrial sites. However, their usage could produce a significant amount of GHG emissions. In 2022, light-duty trucks were the most significant GHG emission source of transportation, contributing to 58% of the total emission of the transportation sector in the U.S. U.S. EPA (2024). Battery electric vehicles (BEVs) play a central role in decarbonizing the transportation sector. Its associated charging infrastructure is currently categorized into two types. The first type is the level 1 and level 2 AC charging (hereafter referred to as 'slow charging'), which generally requires between four hours and a full day to charge a vehicle battery from empty to 80% state of charge (SoC). The second type is the DC fast charging (hereafter referred to as 'fast charging'), available at dedicated stations, which requires a relatively complicated installation process. The fast chargers can recharge an empty vehicle battery to 80% SoC in an hour US Department of Transportation (2025). Fast charging infrastructure also entails considerable capital investments

and installation expenditures, primarily due to the power electronics required. Furthermore, its operational constraints differ from those of slow charging, as charging beyond 80% SoC is strongly discouraged for safety considerations Mussa et al. (2017). Another recharging option is the battery swapping station. The battery swapping station enables EVs to replace depleted batteries with fully charged ones swiftly Mak et al. (2013). However, due to the safety risks associated with battery swapping operations, the feasibility of deploying battery swapping stations at industrial sites should be assessed on a case-by-case basis.

In this paper, we examine the electrification of light-duty trucks at industrial sites for decarbonization. The original diesel-powered trucks are primarily employed for transporting workers and small-scale facilities. The strict operational schedules at industrial sites leave little room for trucks to change any designated parking locations or timetables. As a result, the scheduled trucks are expected to abandon charging if the anticipated waiting time for getting a charger surpasses a specified threshold. This is formulated as a ‘scheduling-with-abandonment’ problem. We conducted a case study of the open-pit mining site with 200 diesel-powered operational trucks. Without modifying any of their GPS data, we extracted their parking and driving patterns based on potential charging points and estimated their energy consumption at half-hour resolutions. Then, we developed a two-stage charging infrastructure planning and scheduling model for the entire truck fleet. The planned EV charging infrastructure satisfies the charging needs of each truck. That is meeting the energy consumption of each truck at any time, given the limited parking durations and battery energy capacity.

1.2. Related Work

1.2.1. Mixed-type charging infrastructure planning Existing studies on charging infrastructure planning primarily focus on determining the location, number, and type of EV chargers, as well as the charging schedule using the selected installation. For electric buses and trucks at industrial sites, the charging process primarily involves opportunity or overnight charging, meaning they are only charged during their layovers and overnight parking Abdelwahed et al. (2020). The vehicle routing is typically not considered in the electric bus scheduling, as buses usually have fixed stop points and timetables. After determining a finite set of candidate locations for potential EV charger deployment based on stop frequency, the number and types of chargers can be optimized according to trip patterns. Hu et al. (2022) models a joint optimization problem for locating fast chargers at selected bus stops and optimizing schedules for opportunity charging. The model assumes that buses will be charged during layovers, and the cost takes into account the time-varying electricity price and penalty for additional waiting times. Legault et al. (2025) formulates a multi-period, integrated planning and scheduling problem. The paper models the electric

bus timetable as a graph representing their charging and driving pattern, which is considered a deterministic, minimum-cost problem. Gkiotsalitis et al. (2025) optimize the EV charger location and number by allocating bus trips to their nearest chargers with available time slots, assuming that buses will be driven to the optimal charger location after the trip ends.

1.2.2. EV charging scheduling with waiting time and abandonment The scheduling problem is a fundamental and widely studied combinatorial optimization problem, with extensive applications in areas such as supply chain management, service management, and healthcare Fonseca et al. (2024), Delarue et al. (2025). EV charging can be viewed as a service that relies on a reusable resource—namely, the charging infrastructure. The EV charging scheduling problem could thus consider different attributes, such as charger availability, charging time, and waiting times for charging services. For instance, the delay or waiting time can be modeled as a monetary penalty in the objective function Hu et al. (2022), Tao et al. (2024), Gkiotsalitis et al. (2025). When the waiting time exceeds a threshold, the vehicle that committed a time-critical task or trip might abandon charging and leave to find another charging spot, which can be represented as a scheduling problem with abandonment G. Chen et al. (2023). Another critical aspect of EV charging is range anxiety, referring to drivers' concern about depleting their battery before reaching a charging station or their destination. Empirical studies suggest that range anxiety may incentivize the installation of additional charging stations or the adoption of larger battery capacities Lim et al. (2015). Lu et al. (2025) model the impact of range anxiety by setting a threshold SoC before reaching the destination. Tao et al. (2024) formulate the accumulated range anxiety level as a function of SoC depletion along the route and integrates the range anxiety into its objective function.

1.2.3. Decision-dependent robust optimization In integrated charging infrastructure planning and scheduling problems, several uncertainties arise, including EV arrival and departure times, charging durations, and energy consumption. They can be modeled using stochastic optimization (SO), robust optimization (RO), and distributionally robust optimization (DRO). Among these formulations, RO typically ensures the highest level of reliability, making it particularly suitable for critical infrastructure planning. Different shapes of uncertainty sets, such as box or ellipse, lead to the robust counterparts and tractability Bertsimas & Hertog (2022). Hu et al. (2022) model the uncertainty of passengers' boarding and alighting time during bus trips using box and budget uncertainty sets based on the RO formulation. L. Chen et al. (2024) conduct EV charging scheduling considering the stochastic arrival time of different user groups, where an exponential cone programming formulation is introduced to approximate the upper bound of the stochastic problem. Y. Chen & Liu (2023) developed a two-stage stochastic model for planning and operating

shared autonomous EV systems, where scenarios represent uncertain user trip requests. An accelerated two-phase Benders decomposition-based algorithm is proposed for solving this two-stage programming problem.

However, these constructed uncertainty sets model uncertainties independent of exogenous factors such as charging decisions. A number of charging installation trials have already shown that charging decisions are very likely to impact parking and waiting durations. For instance, parking duration is strongly correlated with the charging types (e.g., whether it is slow or fast charging) Cui et al. (2023), Zhang et al. (2025). This could be modeled as the decision-dependent uncertainty set, and its uncertainty is endogenous Nohadani & Sharma (2018). Nohadani & Sharma (2018) demonstrates that, in general, RO problems with decision-dependent uncertainty are NP-complete and require either global optimization or reformulation techniques such as the big-M method. Similarly, Noyan et al. (2022) introduces a decision-dependent ambiguity set in a machine scheduling problem and examines how different types of uncertainty dependence affect the model formulation. Their findings show that incorporating affine dependency on decision variables can reduce nonlinear constraints through the use of McCormick envelopes and the big-M approach.

	Decision Variables				User Behavior		Uncertainty formulation
	Location	Number	Scheduling	Type	Waiting time	Range Anxiety	
Abdelwahed et al. (2020)			✓				D
Hu et al. (2022)	✓	✓	✓		✓		RO
Y. Chen & Liu (2023)	✓	✓	✓	✓			SO
L. Chen et al. (2024)			✓				SO
Tao et al. (2024)	✓				✓	✓	D
Lu et al. (2025)			✓			✓	SO
Legault et al. (2025)	✓	✓	✓	✓			D
Gkiotsalitis et al. (2025)	✓	✓	✓	✓	✓		D
Our paper	✓	✓	✓	✓	✓	✓	RO

Notes: D = Deterministic model; RO = Robust Optimization; SO = Stochastic Optimization.

All the aforementioned work about charging infrastructure planning and scheduling is presented in Table 1.2.3. Compared to these works, our paper makes the following contributions:

- We developed a two-stage EV charger planning model that optimizes the charger location, quantity, type, and scheduling. The model introduces a scheduling-with-abandonment formulation that reflects the industrial site's strict operational rules and captures the impacts of overnight parking, range anxiety, and waiting times on the charging scheduling.
- We developed a decision-dependent uncertainty set to capture the variability in parking durations and their differences across charger types (i.e., slow and fast chargers). Although decision-dependent robust optimization models are typically nonlinear, we demonstrated that the proposed affine dependence on the binary charging decision can be linearized, allowing the problem to be formulated as a MILP.

- Considering the high computation cost of the scheduling problem over a long optimization horizon, we designed a ‘fix-and-optimize’ heuristic method to forecast parking intervals with high charging demands in the scheduling. Using the representative days or iterative planning by month, the model achieves an optimality gap of less than 0.1% within a reasonable computation time under four uncertainty scenarios.

2. Problem formulation

2.1. Problem description

The problem is formulated as a two-stage model: the first stage determines charger installations, and the second stage schedules truck charging based on the installed infrastructure. We consider a fleet of electric light-duty trucks $i \in \mathcal{I}$ operating around an industrial site based on the fixed stop points and schedules. As shown in Figure 1, a truck i can be charged during its available half-hour parking time slots $\mathcal{S}_{i,d,t}$ at time t on day d at a charging zone z . One truck cannot appear in more than one zone at a time.

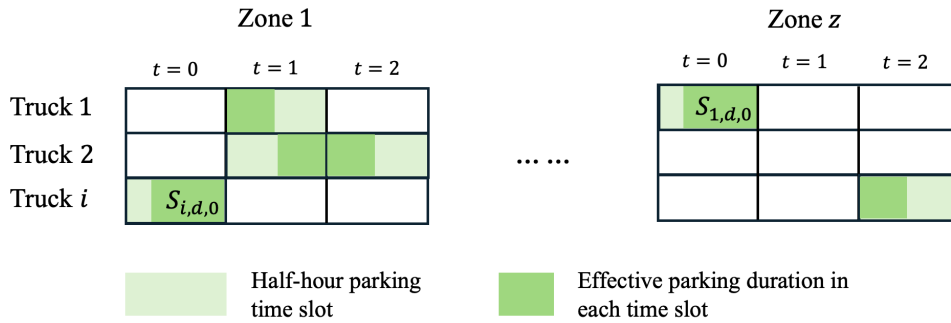


Figure 1 The studied multi-zone charging scheduling problem for the light-duty truck fleet; At any half-hour parking time slot \mathcal{S} shown in light green, a truck can either choose to wait, abandon charging, or charge. The effective parking durations pp are shown in dark green.

Within a parking slot $S_{i,d,t}$, a truck may either wait to be charged, abandon charging, or charge directly using one of the available charger types $j \in \mathcal{J}$. In each parking time slot, the effective parking duration is less than half an hour, which restricts the maximum amount of energy that can be charged for this truck during this parking time window. Across the optimization horizon, the total energy of each truck scheduled to be charged must satisfy the truck’s trip-related energy consumption, considering the battery energy balance, battery SoC constraints, and charging power constraints. The traveling distance and energy consumption during parking slots $S_{i,d,t}$ is not considered. Furthermore, at any time t on the day d , the number of chargers simultaneously used in zone z in type j cannot exceed the number of this type of chargers installed in the zone, x_z^j .

2.2. Set, index, and parameters

- \mathcal{J}, j : Set, index of EV charger types.
- \mathcal{Z}, z : Set, index of EV charging zones.
- \mathcal{I}, i : Set, index of electric trucks.
- \mathcal{D}, d : Set, index of days in the planning horizon.
- \mathcal{T}, t : Set, index of hours in day d .
- $\mathcal{S}_{i,d,t}$: Set of discrete possible parking times for truck i on day d at the time t .
- E_i^{bat} : Battery energy capacity (kWh) of truck i .
- SoC^{max} : Maximum SoC of EV batteries.
- SoC^{min} : Minimum SoC of EV batteries.
- P^j : Power rating (kW) of charger type j .
- η^j : Charging efficiency of charger type j .
- $\rho_{i,d,t}$: Energy consumption usage (kWh) of truck i at time t on day d .
- C_j^{install} : Installation cost for charger type j .
- P^{low} : Penalty for low SoC inducing the range anxiety
- P^{charging} : Penalty for charging time of trucks.
- μ : Mean of parking durations by truck i at hour t at zone z across all the optimized days.
- σ : Standard deviation of parking durations by truck i at hour t on day d at zone z across all the optimized days.
- Δt : Duration (mins) in each parking time interval

2.3. Decision variables

- $x_z^j \in \mathbb{Z}^+$: The number of chargers of type j installed in zone z .
- $w_{i,d,t} \in \mathbb{R}^+$: Accumulated waiting time for truck i at charger j on day d at time t .
- $b_{i,d,t} \in \mathbb{R}^+$: Battery SoC level (%) of truck i at time t on day d .
- $p_{i,d,t} \in \mathbb{R}^+$: EV charging power (kWh) of truck i at time t on day d .
- $v_{i,d,t} \in \mathbb{R}^+$: Battery SoC inadequacy below the low SoC threshold.
- $T_{i,d,t}^{\text{max}} \in \mathbb{R}^+$: Maximum waiting time before truck i abandons charging at time t on day d .
- $\delta_{i,d,t}^{30} \in \{0, 1\}$: Indicator for the lower SoC bound of EV batteries inducing range anxiety.
- $y_{i,d,t}^j \in \{0, 1\}$: Binary variable indicating that truck i is charged with charger type j at time t on day d (1 for charging and 0 for not).
- $a_{i,d,t} \in \{0, 1\}$: Binary variable indicating that truck i abandons charging at time t on day d (1 for abandonment and 0 for not).

2.4. Uncertainty variables

- $pp_{i,j,z,t} \in \mathbb{R}^+$: Parking duration for truck i at time t in zone z using charging type j .

2.5. Objective function

The objective function consists of two stages: the charging planning and scheduling stages. The planning stage considers multiple types of charging infrastructure, such as slow and fast chargers. In addition to power capacity, we also model the SoC charging range for each type of charger, which is detailed in the following section. The operational part includes penalties for low battery SoC, which induces range anxiety and affects charging time during scheduling.

$$\min \underbrace{\sum_{j \in \mathcal{J}} \sum_{z \in \mathcal{Z}} C_j^{\text{install}} \cdot x_{z,j}}_{\text{Installation cost of mixed-type EV chargers}} + \underbrace{P^{\text{low}} \sum_{i \in \mathcal{I}} \sum_{d \in \mathcal{D}} \sum_{t \in \mathcal{T}_d} v_{i,d,t}}_{\text{Penalty for low SoC of EV batteries}} + \underbrace{P^{\text{charging}} \sum_{i \in \mathcal{I}} \sum_{d \in \mathcal{D}} \sum_{j \in \mathcal{J}} \sum_{t \in \mathcal{T}_d} y_{i,d,t}^j}_{\text{Penalty for EV charging time}}$$

where the low SoC penalty is calculated as the sum of the soft violation variable $v_{i,d,t} := [0.3 - b_{i,d,t}]^+$. This variable is greater than zero (i.e., $v_{i,d,t} > 0$) if and only if the battery SoC level falls below 30 %. The charging time penalty is calculated as the sum of all the charging times across all zones and the time horizon to prevent low charger utilization.

2.6. Constraints for charging planning and scheduling

The following subsections detail constraints pertaining to charging planning and scheduling for the entire fleet of electric trucks. We also introduced three big-M constraints, and we discussed the range value of these M in Appendix B.

2.6.1. Truck charging constraints We impose the following constraints to govern the truck charging behavior:

$$(\text{Single charger usage}) \quad \sum_{j \in \mathcal{J}} y_{i,d,t}^j \leq 1 \quad \forall i, d, t \quad (1)$$

$$(\text{Charging only in parking windows}) \quad y_{i,d,t}^j = 0 \quad \forall i, t \notin \mathcal{S} \quad \forall j \quad (2)$$

$$(\text{Low SoC indicator}) \quad \begin{aligned} b_{i,d,t} - \frac{30}{100} &\geq -M_1 \cdot \delta_{i,d,t}^{30} + \epsilon \\ b_{i,d,t} - \frac{30}{100} &\leq M_1 \cdot (1 - \delta_{i,d,t}^{30}) \quad \forall i, d, t. \end{aligned} \quad (3)$$

Constraint (1) ensures each truck uses at most one charger at any time. Constraint (2) enforces charging only during the scheduled parking window. Constraint (3) defines the binary indicator $\delta_{i,d,t}^{30}$ for the low SoC condition, where $\delta_{i,d,t}^{30} = 0$ if and only if the battery level exceeds 30%. Here, M_1 is a large constant, and the effective range of M_1 is presented in Appendix B. The parameter ϵ is a small positive number, and it ensures that the indicator equals one only when the battery SoC is strictly greater than 30%, thereby guaranteeing a unique waiting time when the battery SoC is exactly 30%.

2.6.2. Abandonment and waiting time constraints We model two coupled phenomena during each half-hour parking slot t on day d : (i) *abandonment*—once a driver gives up waiting, no charging may occur in that slot; and (ii) *waiting-time accumulation*—while a truck remains parked in the *same zone* across consecutive admissible slots and is not charging, its waiting time increases by Δt ; otherwise it resets to zero.

Abandonment Let $a_{i,d,t} \in \{0,1\}$ indicate that truck i abandons in slot (d,t) and let $y_{i,d,t}^j \in \{0,1\}$ be the charger-type assignment. We enforce

$$(\text{Once abandon, no charging}) \quad a_{i,d,t} \leq 1 - \sum_{j \in \mathcal{J}} y_{i,d,t}^j, \quad \forall i, d, t, \quad (4)$$

so choosing abandonment excludes charging in that slot. During a continuous parked stretch (defined below), the abandonment variable is non-decreasing:

$$a_{i,d',t'} \geq a_{i,d,t}, \quad \forall (d', t') \text{ successor of } (d, t). \quad (5)$$

(Persistence over a parked stretch: once abandoned, a truck remains abandoned in subsequent slots within the same zone.)

Waiting time Let $w_{i,d,t} \geq 0$ be the accumulated waiting time upon entering slot (d,t) . When two consecutive admissible slots for truck i occur in the *same zone*, waiting evolves as

$$(\text{Within-zone recursion}) \quad w_{i,d,t+1} = w_{i,d,t} + \Delta t \left(1 - \sum_{j \in \mathcal{J}} y_{i,d,t}^j \right), \quad \forall i, d, t \text{ with same-zone successor}, \quad (6)$$

i.e., w grows by Δt only if the truck was *not* charging in the preceding slot. Otherwise, w resets:

$$(\text{Resets}) \quad w_{i,d,t} = 0, \quad \begin{array}{l} \text{if } (i, d, t) \text{ is not an admissible parking slot;} \\ \text{or if the predecessor admissible slot is in a different zone.} \end{array} \quad (7)$$

Rule (7) initializes w at the start of any parked stretch and breaks carryover across zone changes; Equation (6) propagates w across day boundaries when the zone is unchanged (e.g., from (d, T_d-1) to $(d+1, 0)$). Two special cases for resetting the waiting time, the day-to-day carryover of waiting time in the same zone and zone-change reset of waiting time, are presented in Figs. 2 and 3, respectively. The full illustration of waiting time and abandonment is presented in Appendix A.

2.6.3. Charging abandonment rules At an industrial site, a truck abandons charging if its waiting time exceeds a maximum allowed waiting time $T_{i,d,t}^{\max}$, as constraint (8). M_2 is a large constant to relax the waiting time constraint when $a_{i,d,t}$ equals to 1, in other words, when the trucks abandon charging. Notably, the maximum waiting time is a variable and it depends on the truck SoC due to the range anxiety and whether it is parked in special zones that allow for the overnight charging.

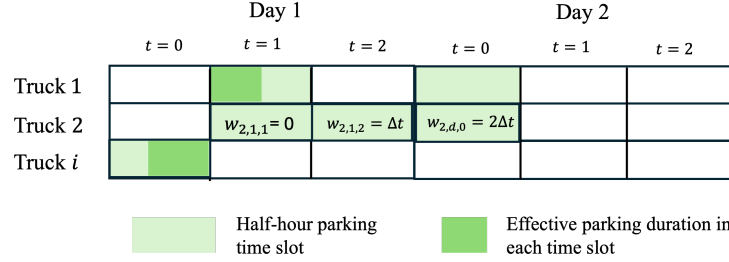


Figure 2 Day-to-day carryover of waiting time in the same zone. For Truck 2 on Day 1, the first admissible slot initializes $w = 0$. The next slot in the same zone accumulates to $w = \Delta t$, and carryover to Day 2 in the same zone yields $w = 2\Delta t$.

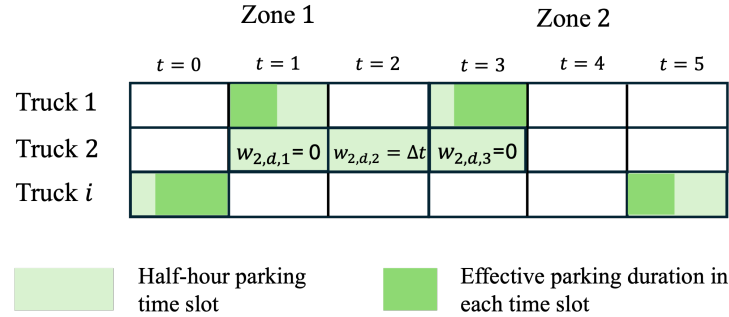


Figure 3 Zone-change resets of waiting time. For Truck 2, waiting grows from $w = 0$ to $w = \Delta t$ across two slots in Zone 1. Transition to Zone 2 resets $w = 0$, after which accumulation resumes in subsequent uncharged slots.

Based on experiences from the industrial partner, we formulate the following waiting and abandonment rules, considering range anxiety and overnight charging in the special zones. As constraint (9), if the SoC is greater than or equal to 30%, no waiting time is allowed as the driver has no range anxiety. If the SoC of a truck is below 30%, this will result in the driver's range anxiety and would extend their waiting time to 0.5 hours before abandoning charging. Let the set S^Z denote the parking time slots at any of the special zones for overnight charging. Constraint (10) sets the waiting time to be zero when the truck is outside the parking windows (i.e., no parking allowed) or in special zones (i.e., no waiting time limits). Constraint (11) regulates that the waiting time is always non-negative.

$$(\text{Abandon after the maximum waiting time}) \quad w_{i,d,t} \leq T_{i,d,t}^{\max} + M_2 \cdot a_{i,d,t} \quad \forall i, d, t \in \mathcal{S} \quad (8)$$

$$(\text{Maximum waiting time in non-special zones}) \quad T_{i,d,t}^{\max} = \Delta t \cdot \delta_{i,d,t}^{30} \quad \forall i, d, t \in \overline{\mathcal{S}^Z} \quad (9)$$

$$(\text{Outside parking windows or in special zones}) \quad w_{i,d,t} = 0 \quad \forall i, d, t \in \mathcal{S}^Z \cup \overline{\mathcal{S}} \quad (10)$$

$$(\text{Non-negative constraint}) \quad w_{i,d,t} \geq 0 \quad \forall i, d, t \in \mathcal{S} \quad (11)$$

2.6.4. Battery dynamics constraints We impose the following constraints to model battery SoC evolution and charging power limits:

$$(\text{Battery energy balance}) \quad b_{i,d,t} E_i^{bat} = b_{i,d,t-1} E_i^{bat} + p_{i,d,t}^{ch} - \rho_{i,d,t}, \quad \forall i, d, \forall t \geq t_0 \quad (12)$$

$$(\text{The initial and final SoC are equal}) \quad b_{i,d_0,t_0} = b_{i,d_e,t_e} \quad \forall i, d, t \quad (13)$$

$$(\text{Maximum charging power limit}) \quad p_{i,d,t}^{ch} \leq \sum_{j \in \mathcal{J}} \eta^j \cdot P^j \cdot \Delta t \cdot y_{i,d,t}^j \cdot pp_{i,d,t}, \quad \forall i, d, t \in \mathcal{S} \quad (14)$$

$$(\text{Effective charging time limits}) \quad \frac{5}{30} \leq pp_{i,d,t} \leq 1, \quad \forall i, d, t \in \mathcal{S} \quad (15)$$

$$(\text{Battery SoC limits}) \quad \text{SoC}^{\min} \leq b_{i,d,t} \leq \text{SoC}^{\max} \quad \forall i, d, t \quad (16)$$

Constraint (12) models EV battery dynamics considering charging power and energy consumption, and it should be noted that we do not use a binary variable to model battery discharging status, as it shall not happen during parking. Constraint (13) sets the initial SoC at t_0 and final SoC at time t_e of the optimization horizon to be the same. Constraint (14) sets the maximum charging power limit considering the charging type P^j and corresponding charging efficiency η^j . Constraint (15) regulates the charging time limit in each time window, which is greater than 5 mins and less than 30 minutes. Finally, constraint (16) restricts battery SoC within the maximum and minimum values.

2.6.5. Fast charger SoC restrictions To prevent trucks from using fast chargers when their SoC exceeds 80% and to ensure that fast chargers do not charge the battery SoC beyond 80%, the following constraints are enforced when charging. Constraint (17) ensures that if $b_{i,d,t} > 80\%$, then $\delta_{i,d,t}^{80} = 1$, and $y_{i,d,t}^1 = 0$, preventing the use of the fast charger. Also, if $b_{i,d,t} \leq 80\%$, then $\delta_{i,d,t}^{80} = 0$, allowing the fast charger to be used. Constraint (18) ensures that when the fast charger is used, the battery level after charging ($b_{i,d',t'}$) is limited to at most 80%.

$$(\text{SoC cap before fast charging}) \quad b_{i,d,t} \leq \frac{80}{100} + M_3 \cdot (1 - y_{i,d,t}^1) \quad \forall i, d, t \in \mathcal{S} \quad (17)$$

$$(\text{SoC cap during fast charging}) \quad b_{i,d',t'} \leq \frac{80}{100} + M_3 \cdot (1 - y_{i,d,t}^1) \quad \forall i, d', t' \in \mathcal{S} \quad (18)$$

Here, $b_{i,d,t}$ is the SoC of truck i ; $y_{i,d,t,1}$ is a binary variable equal to 1 if truck i uses a fast charger at time t on day d ; M_3 is a large constant; and \mathcal{S} is the set of time steps t on day d when truck i is parked. The pair (d', t') represents the next time step after (d, t) , defined as $(d, t+1)$ if $t < T-1$, or $(d+1, 0)$ if $t = T-1$ and $d < D-1$, where T is the number of time steps per day and D is the number of days.

2.6.6. Decision-dependent uncertainty sets of parking duration The effective charging duration $\hat{p}p$ is stochastic and influenced by the charging decision $y_{i,d,t}^j$, which is represented as binary variables. We constructed a box-shaped, decision-dependent uncertainty set for truck i in zone z at hour t . This is formulated as a robust linear constraint with affine decision dependence in terms of charging decisions, $y_{i,t,z}^j$.

$$p_{i,d,t}^{ch} \leq \sum_{j \in \mathcal{J}} \eta^j \cdot P^j \cdot \Delta t \cdot y_{i,d,t}^j \cdot \hat{p}p_{i,t,z}, \quad \hat{p}p \in \Phi(y_{i,t,z}^j) \quad \forall i, d, t \in \mathcal{S} \quad (19)$$

The box-shaped uncertainty set $\Phi(y_{i,t,z}^j)$ is defined as,

$$\Phi = \left\{ \hat{p}p \in \mathbb{R}^{i \times t} \mid \frac{5}{30} \leq \hat{p}p \leq 1, \mu_{i,t,z}(y_{i,t,z}^j) - \sigma_{i,t,z}(y_{i,t,z}^j) \leq \hat{p}p \leq \mu_{i,t,z}(y_{i,t,z}^j) + \sigma_{i,t,z}(y_{i,t,z}^j) \right\} \quad (20)$$

Where the bounds of the uncertainty set depend on the the minimum and maximum charging time, and calculated mean $\mu_{i,t,z}$ and standard deviation $\sigma_{i,t,z}$ associated with the charging decisions. The nominal moments are extracted from the historical data. Many charging trial data shows that fast charging could reduce the uncertainty of parking duration as the charging time becomes short. Therefore, we introduced a factor γ to represent the reduction in uncertainty resulting from the fast charger usage.

$$\mu_{i,t,z}(y_{i,t,z}^j) := \hat{\mu}_{i,t,z}(y_{i,t,z}^0 + y_{i,t,z}^1) \quad (21)$$

$$\sigma_{i,t,z}(y_{i,t,z}^j) := \hat{\sigma}_{i,t,z}(\gamma^0 \cdot y_{i,t,z}^0 + \gamma^1 \cdot y_{i,t,z}^1) \quad (22)$$

Where y^0 and y^1 indicate charging decisions using slow or fast chargers, respectively. Notably, the decision-dependent RO is NP-complete, non-linear due to the multiplication of variables Nohadani & Sharma (2018). Here we proved that the proposed formulation is a special case that can be formulated as a robust linear constraint (31), and therefore the model can be formulated as a MILP problem. The proof is presented in Appendix C.

$$p_{i,d,t}^{ch} \leq \sum_{j \in \mathcal{J}} \eta^j \cdot P^j \cdot \Delta t \cdot (\hat{\mu}_{i,t,z} \cdot y_{i,d,t}^j - \hat{\sigma}_{i,t,z} \cdot \gamma^j \cdot y_{i,t,z}^j), \quad \forall i, d, t \in \mathcal{S} \quad (23)$$

2.6.7. Total number of chargers in each type and zone The number of trucks charging with charger type j cannot exceed the number of available chargers of type j in zone z at any time.

$$\sum_{i \in \mathcal{I}} y_{i,d,t}^j \mathbb{1}\{\text{truck } i \text{ at zone } z \text{ at time } t, \text{ day } d\} \leq x_z^j \quad \forall z \in \mathcal{Z}, \forall j \in \mathcal{J}, d \in \mathcal{D}, t \in \mathcal{T} \quad (24)$$

Where $\mathbb{1}$ is a binary indicator to represent whether truck i is at zone z at time t of day d .

3. Robust planning using the whole year dataset

The planned EV infrastructure must remain robust across the year-round fleet operations. We compare two approaches to solving based on the whole-year dataset: day selection (DS) and iterative planning and scheduling (IPS).

- DS: We selected a certain number of representative days based on statistical criteria, such as the total fleet distance, the number of moving trucks, the total fleet energy consumption, and the total stopping time during a day. We also included days around the representative days to preserve the trip and battery cycle continuity.
- IPS: We first decomposed the full-year dataset into monthly subsets, allowing several overlapping days between months. The algorithm then plans charger deployment for the entire year by iteratively integrating scheduling and monthly planning. It starts with an initial charger allocation derived from the dataset and processes each month sequentially. If the existing infrastructure can satisfy the charging demand of this month, only charging scheduling is performed. Otherwise, the algorithm jointly determines the charging schedule and the additional chargers required, updates the infrastructure, and carries the new configuration forward to subsequent months.

4. Fix-and-optimize heuristic based on high charging demand forecasts

Directly solving the proposed planning and scheduling model can be computationally demanding with a long optimization horizon. In this paper, we propose a fix-and-optimize heuristic designated for the scheduling problem based on high charging demand forecasts. The fix-and-optimize heuristic has been applied to timetable Fonseca et al. (2024) and job-shape scheduling Li et al. (2025) problems, where part of the solution is fixed while the remaining variables are free to form subproblems. In this paper, as presented in Fig. 4, we identified the parking intervals with high charging demand at an early stage based on the samples from the uncertainty set and pre-assigned fast-charging schedules, thereby accelerating the overall optimization process.

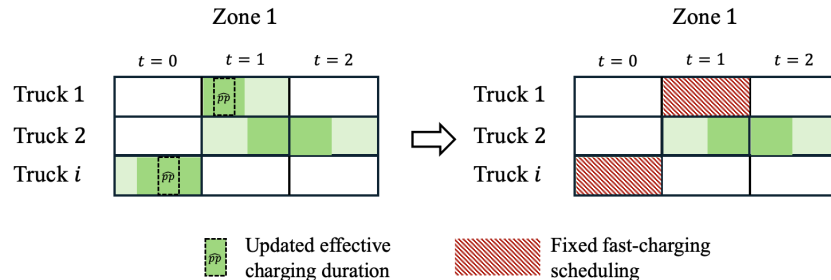


Figure 4 The fix-and-optimize heuristic where fast-charging scheduling is pre-assigned and fixed based on the forecast high charging demands

As shown in Algorithm 1, we first initialize the master problem using the starting values $pp_{i,d,t}$ to solve the model. Next, we sample the stochastic parking duration $\hat{pp}_{i,d,t}$ from the uncertainty set $\Phi(\mu, \epsilon)$ to replace the initial values and compute the upper bounds of the charging power based on these samples. We then compare the required charging power against the updated upper bounds to identify any violations. A violation occurs if the required charging power exceeds the upper bound by more than a threshold κ^v and the parking window does not belong to a special zone. The threshold κ^v is initialized at two and decays exponentially across iterations. When a violation is detected, a fast-charging scheduling constraint $y_{i,1,d,t} = 1$ is added for that parking window. These constraints are subsequently incorporated into the master problem, after which the model is reset and resolved from the first step.

Algorithm 1: Fix-and-optimize heuristic under effective parking duration uncertainty

Input: Parking duration samples $\hat{pp}_{i,d,t}$ drawn from the uncertainty set $\Phi(\mu, \epsilon)$

Output: Charger installation decisions x_z^j

repeat

Solve the proposed optimization problem with deterministic $pp_{i,d,t}$ as the initial input (master problem); \triangleright *Warm start if the solution of the master problem available;*

Obtain scheduling outcomes $y_{i,j,d,t}$ and charging profiles $p_{i,j,d,t}^{ch}$;

Sample parking durations $\hat{pp}_{i,d,t}$ from the uncertainty set $\Phi(\mu, \epsilon)$;

for $i \in \mathcal{I}$, $t \in \mathcal{T}$, $d \in \mathcal{D}$, $j \in \mathcal{J}$ **do**

Compute the new upper bound of charging power:

$$p_{i,j,d,t}^{ch'} \leftarrow \sum_{j \in \mathcal{J}} \Delta t \cdot P^j \cdot y_{i,j,d,t} \cdot \hat{pp}_{i,d,t} \cdot \eta^j$$

if $(p_{i,0,d,t}^{ch} \geq p_{i,0,d,t}^{ch'} + \kappa^v) \wedge (\forall i, d, t \in \overline{\mathcal{S}^Z})$ **or** $p_{i,1,d,t}^{ch} \geq p_{i,1,d,t}^{ch'}$ **then**

Impose the fast-charging constraint $y_{i,1,d,t} = 1$ in the master problem;

until *The maximum iteration limit is reached;*

Post-process the solution by removing fast charging results in zones where the number of fast chargers exceeds two;

Re-solve the optimization problem using the sampled values $\hat{pp}_{i,d,t}$ and incorporating the charger installation constraints derived from the processed solution;

This iterative process continues until the maximum number of iterations is reached. Afterward, we post-processed the optimization results by removing zones with more than two fast chargers. The remaining fast charger installations were treated as hard constraints, while the solutions for slow chargers were used as lower bounds. Ultimately, the installation plan for all zones and charger types was determined.

5. Application

We applied our model to an open-pit mining site with 203 light-duty trucks in operation, which are planned to be replaced by battery EVs. Seven special-use trucks, such as ambulances, that will not be electrified, along with another seven trucks dispatched fewer than 10 days, are excluded

from the study. The remaining 189 trucks will be replaced with electric trucks equipped with 100 kWh batteries. We consider the following two types of chargers, as listed in Table 1. The capital cost of fast chargers includes the installation cost. We set the penalty of low SoC and charging time to be one in the objective function. The charging efficiency could vary with the charging type, outdoor temperature, and charging power Sevdari et al. (2023). This paper uses a fixed value for charging efficiency. Overall, fast charging tends to be more efficient than slow charging, as it uses a high-efficiency rectifier located outside the truck Arena et al. (2024). We therefore set the charging efficiency of slow and fast charging to be 90% and 95%.

Specifications	Slow charger	Fast charger
Capital costs (\$/charger)	1,500 Ford (2025)	38,000 Primecomtech (n.d.)
Maximum charging rates (kW)	11.2	150
SoC ranges	10–100%	10–80%
Charging efficiency	90% Sevdari et al. (2023)	95% Arena et al. (2024)

Table 1 Technical parameters of two types of EV chargers

The charging planning process begins by identifying potential charging sites based on the stop frequency of all trucks (Section 5.1). Next, the parking window, effective parking duration, and energy consumption for each truck are extracted (Section 5.2). Using this information, the DS and IPS methods are applied to plan across the full-year horizon. If the RO formulation is used, a decision-dependent uncertainty set is constructed from the historical samples (Section 5.3). High-consumption vehicles with infeasible trips are then filtered out (Section 5.4). Finally, chargers are planned through the proposed model in the deterministic or stochastic formulation (Section 5.5).

5.1. Identifying potential EV charging points

We used GPS records of 189 light-duty trucks at the mining site over one year. Their GPS data records include coordinates (i.e., longitude and latitude) and speed at each time step. We then grid-divided the entire mining site into 100-meter \times 100 100-meter square regions and counted the stop frequency in each square. We assumed that a truck stops if it moves less than 50 meters within a square region for at least five minutes. Comparing the number of stop frequencies in each square, we identified eight EV charging points with the highest number of stops throughout the year. Fig. 5 shows eight EV charging points identified, and the dashed gray lines indicate the roads connecting them. Fig. 6 shows the total stopping time of the entire fleet (\times 1,000 hours), including both short parking durations (< 4 hours) and long parking durations (≥ 4 hours), along with the annual number of trucks stopping at each zone. The detailed statistics of eight charging zones are listed in Table 6 in Appendix D.1. The zone 1 (roadhouse) and zone 4 (equipment maintenance) have a large part of long duration time greater than 4 hours, which means that most of the overnight parking happens at zones 1 and 4.

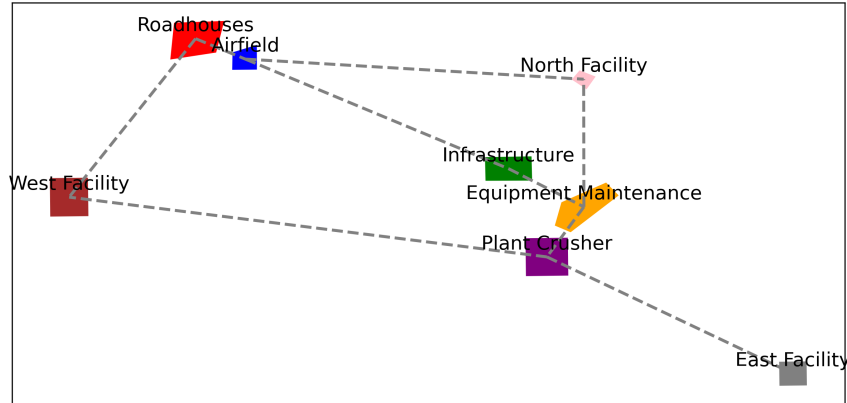


Figure 5 Identified eight charging zones and roads connected to eight charging zones (indicated as gray dashed lines)

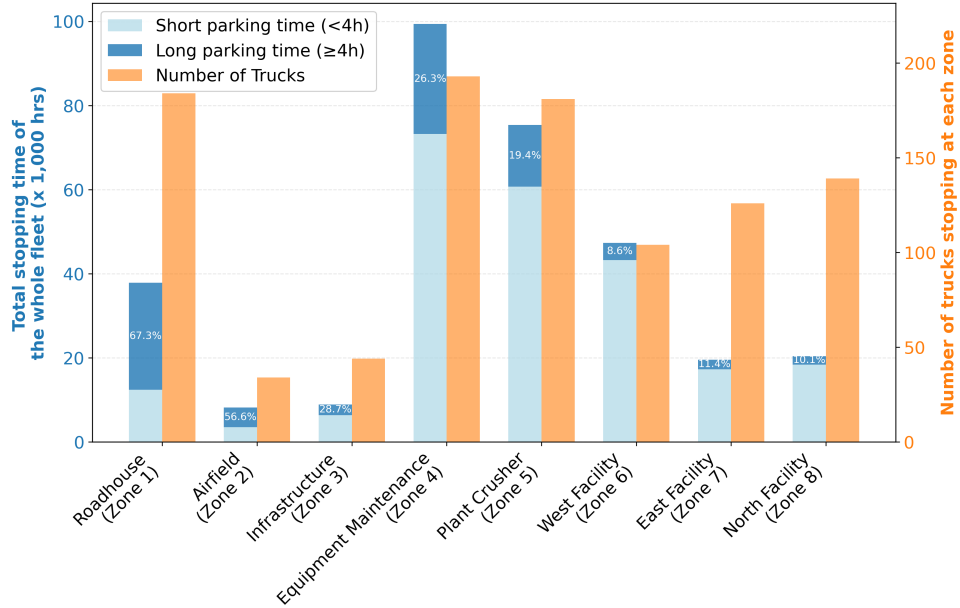


Figure 6 The total stopping time of the entire fleet ($\times 1,000$ hours), including both short parking durations (< 4 hours) and long parking durations (≥ 4 hours), along with the annual number of trucks stopping at each of eight zones

5.2. Summary of input datasets

We extracted three inputs for each truck in each half-hour interval based on their GPS records: (i) the travel distance of each truck in miles, (ii) the parking time windows as the input of the set $\mathcal{S}_{i,d,t}$, and (iii) the effective parking duration in each time window in minutes as the input of $pp_{i,d,t}$. The travel distance is then converted to energy consumption for each half-hour parking time window based on the second-order model of the temperature-dependent fuel economy for U.S.

trucks Goodall & Robartes (2024), as the input of $\rho_{i,d,t}$. The detailed procedures to extract all three kinds of inputs are illustrated in Appendix D.3.

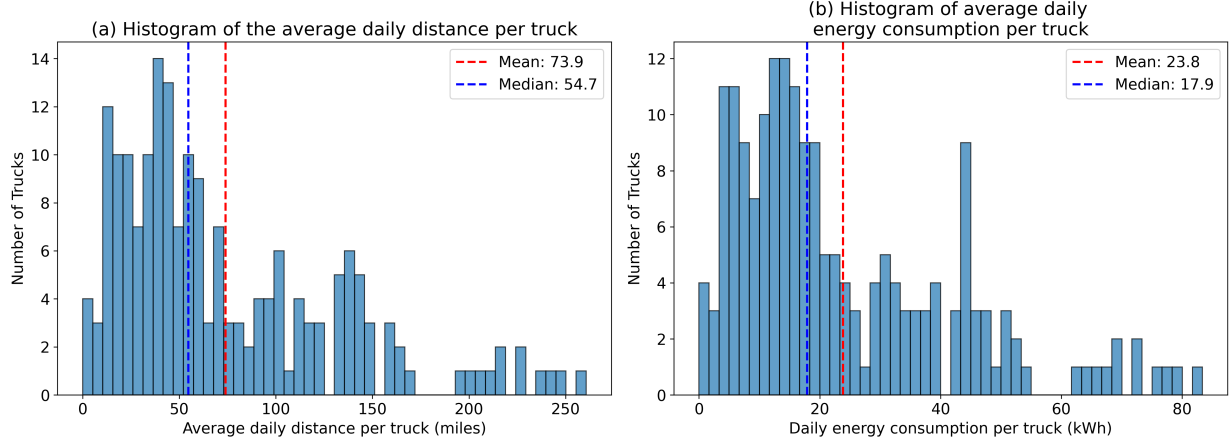


Figure 7 (a) The histogram of average daily distance per truck (miles) and (b) the histogram of average daily energy consumption per truck (kWh)

Figs. 7 (a) and (b) illustrate the distributions of average daily distance traveled per truck and the corresponding average daily energy consumption. On average, each truck traveled 73.9 miles per day. With a fuel economy of roughly 3–3.4 miles/kWh, this translates to a daily energy use of 22.4–24.6 kWh per truck, or about 30% of the battery’s capacity. This implies that a full battery cycle would typically last 2–3 days. It is important to note that travel distance and energy consumption within charging zones are excluded from the model. We expect, however, that this additional consumption could be offset with minor operational adjustments, such as modifying parking durations.

5.3. Samples for constructing robust uncertainty sets

To construct a robust uncertainty set for heterogeneous effective parking durations, we first collected all parking durations and parking window data across the year. Fig. 8 (a) illustrates the total time of actual parking duration versus the the total time of the full parking window per truck per day at eight zones. In each zone, a portion of the parking window cannot be used for charging, for example, when the truck is moving to find a parking spot. Fig. 8 (b) presents the distribution of parking durations across eight zones, showing that zones 6, 7, and 8 exhibit greater variability compared to the others.

We found that the actual parking duration at the mining site is strongly related to trucks, hour of the day, and charging zones, but has almost no correlation with day of the week or day of the

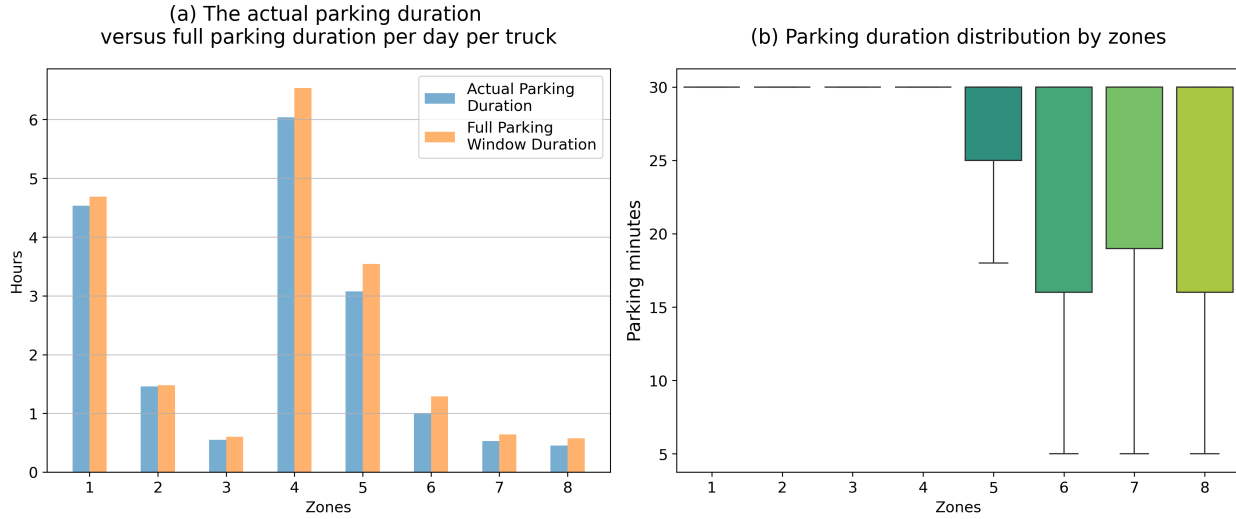


Figure 8 (a) Actual parking duration versus full parking windows duration per day per truck and (b) box plots of actual parking duration distributions of eight zones

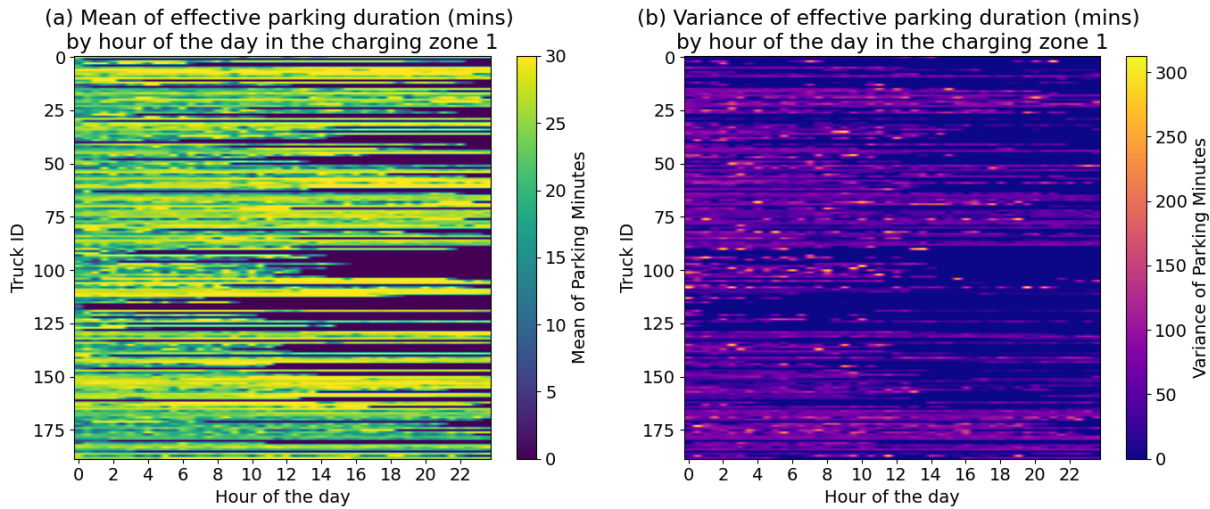


Figure 9 (a) Mean and (b) variance of effective parking durations in minutes of 189 trucks by hour of the day in the charging zone 1

month. This is because the mining site operates continuously with the same pattern throughout the year. We then calculate the mean and standard deviation of parking durations pertaining to trucks, hours of the day, and zones. Fig. 9 shows the mean and variance of effective parking duration in minutes by hour of the day in the charging zone 1. Most trucks operating around the mining site have zero means and variances in their actual parking duration during the day.

5.4. Set up

We prepared three inputs based on the dataset of the year 2023, for the DS and IPS approaches, respectively. For the DS approach, we defined 10 statistical criteria, including total fleet distance, number of active trucks, and total fleet energy consumption. Based on these criteria, we ranked all 365 days in a year and selected the top-ranking days. We experimented with different numbers of selected days, ranging from 10 to 40, and observed that charger installation results stabilized once the selection reached 30 days. Accordingly, we chose 39 days, including days adjacent to the top 10 ranked days, as some vehicles charge every two or three days, and representative sub-periods need to extend beyond battery cycles. The detailed selection criteria and procedures are provided in Appendix D.2. For the IPS approach, we divided the full-year dataset into monthly subsets, incorporating overlapping days between consecutive months to maintain trip continuity. This procedure produced 12 monthly datasets, each spanning 34 days.

We conduct a preliminary simulation before optimization, in which each EV uses straightforward fast charging throughout the optimization horizon. In each simulation, a truck starts with a random SoC and is then fully charged at each parking site. At the end of the optimization horizon, we track whether they could restore their original SoC. If the original SoC cannot be recovered, the truck is identified as a high consumption vehicle (HCV), which cannot be feasibly electrified if it sticks to the current operational scheduling. This also includes vehicles not passing the eight charging zones. The optimization is subsequently performed exclusively on the rest of the trucks, and we recorded the number of HCVs excluded from the optimization model in each simulation. All experiments were solved using the Gurobi commercial solver. We set the accepted optimal gap for this MILP to be 1%, less than the capital cost of one slow charger. All problems were solved on a computer equipped with an 8-core CPU running at 3.4 GHz and 160 GB of RAM.

5.5. Result evaluation

5.5.1. The impacts of abandonment, range anxiety, and effective parking duration

We first evaluate four deterministic cases to analyze the impacts of charging abandonment, range anxiety, and parking duration restrictions. Using the DS method, we draw on 39 selected representative days for the input datasets. The total energy consumption of the entire vehicle fleet for the 39-day optimization horizon is 83,050 kWh, which is around 11.33 kWh per day per truck. The total parking time of the entire vehicle fleet is 124,639 hours, which is around 17 hours per day per truck.

- **Case 1 - Benchmark:** Trucks are prohibited from waiting in any zone under normal circumstances. However, when a vehicle SoC drops to below 30%, it is permitted to pause for 30 minutes

to recharge. Two designated zones (i.e., zone 1 and zone 4) accommodate the overnight charging with unlimited waiting time. The model incorporates the specific parking duration for each parking window (i.e., $\frac{5}{30} \leq pp \leq 1$).

- **Case 2 - Full parking time:** This case maintains the same conditions as the benchmark case, except that it has no specific parking duration constraints for each parking window (i.e., $pp = 1$).

- **Case 3 - No overnight charging:** This case maintains the same conditions as the benchmark case, except that it has no special zones for the overnight charging.

- **Case 4 - No range anxiety:** This case maintains the same conditions as the benchmark case, except that it has no related constraints or penalty related to the range anxiety, in other words, there is no penalty for low SoC (i.e., $P^{low} = 1$). Trucks are prohibited from waiting in any zone under normal circumstances, regardless of their SoC. In other words, the maximum waiting time is set to zero (i.e., $T_{i,d,t}^{max} = 0$).

Table 2 summarizes optimization results in four deterministic cases under different assumptions about abandonment, range anxiety, and effective parking duration. The benchmark case (case 1) has a mixed type of chargers, which are 72 slow chargers and 7 fast chargers. Compared to the benchmark case, case 2 shows that a less number of fast chargers are needed if the model does not consider effective charging time in each parking time slot. In case 3, an additional number of 20 slow chargers are installed if there is no special zone allowing for overnight charging. In case 4, if the model does not consider range anxiety, seven additional slow chargers need to be installed to accommodate more frequent abandonment without waiting time.

Instances	# of HCVs	# of slow / fast chargers	Installation cost (\$)	Scheduling penalty (\$)	Gap (%)	Time (h)
Case 1	1	72/6	336,000	38,468	0.084	2.98
Case 2	1	74/3	187,000	39,622	0.116	57.32
Case 3	1	92/6	366,000	85,200	0.042	15.77
Case 4	1	79/6	346,500	38,077	0.079	2.94

Table 2 Summary of optimization results in four deterministic cases: benchmark, no parking time restriction, no overnight charging, and no range anxiety

Fig. 10 illustrates the differences in the numbers of fast and slow chargers in cases 2–4, compared with the benchmark. Across four cases, the number of installed chargers is proportional to the total duration of vehicle stops at each charging zone, as presented in Fig. 8 (a), and zones 4 and 5 have the highest number of chargers. In case 1, setting the special zones does not relax the requirement of the fast charger installation in these zones, as in zones 1 and 4. In case 3, without considering the overnight charging, zones 1 and 4 will have a high number of slow chargers. In case

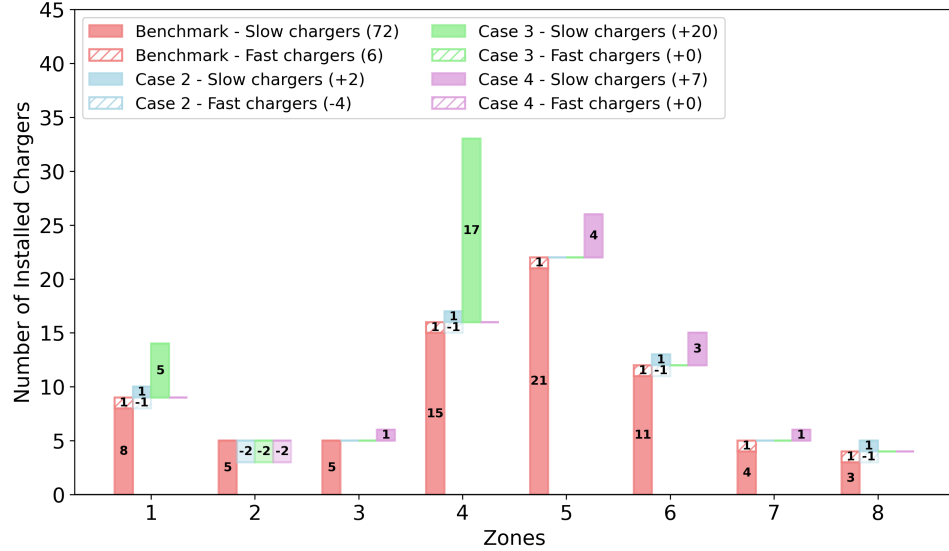


Figure 10 Zone-wise differences in the number of slow and fast chargers of cases 2-4 compared with the benchmark

4, without considering the range anxiety, zones 5-7 will have a higher number of slow chargers, meaning vehicles passing through these three zones have a relatively low SoC than other zones.

Instances	Total slow charging hours	Total fast charging hours	Total abandonment hours	Avg. charging hours (truck per day)	Avg. charging power (kW)
Case 1	3677.0	1352.5	26371.0	0.69	16.51
Case 2	5779.0	555.5	26430.5	0.86	13.11
Case 3	3493.5	1418.5	69353.0	0.67	16.90
Case 4	3116.5	1248.5	26947.0	0.60	19.02

Table 3 Summary of the scheduled charging hours, abandonment hours, and charging power across four deterministic cases

We calculate the charging power, charging hours, and abandonment hours across four deterministic cases, summarized in Table 3. The detailed scheduling solution of four cases are presented in Appendix E. Case 2, which assumes full parking duration, results in the highest total charging hours but the lowest average charging power due to having the fewest fast chargers. Case 3, which excludes overnight charging, produces the greatest number of abandonment hours. Case 4, which removes range anxiety, leads to the fewest charging hours and the highest average charging power.

Figs. 11 (a) and (b) show the zone-wise comparison of charging and abandonment time, respectively. In case 2, with the full parking duration, zones 6 and 8 have a higher charging time. In case 3, without the overnight charging, zones 1 and 4 have a significantly high number of abandonment hours. Figs. 12 (a) and (b) show the total number of charging and abandonment hours of the total

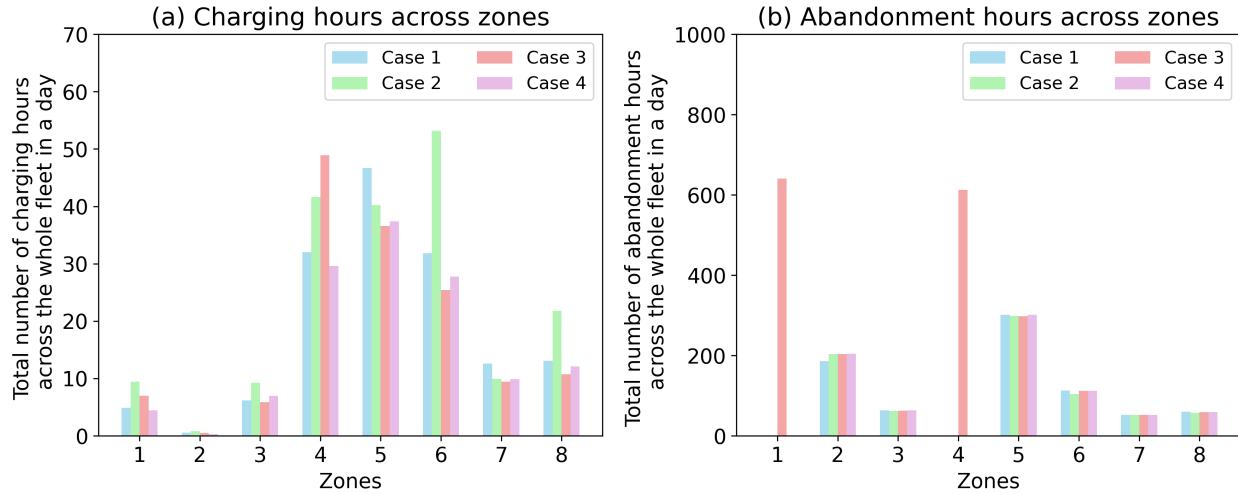


Figure 11 The total number of (a) charging hours and (b) abandonment hours of the entire truck fleet in a day across four instances

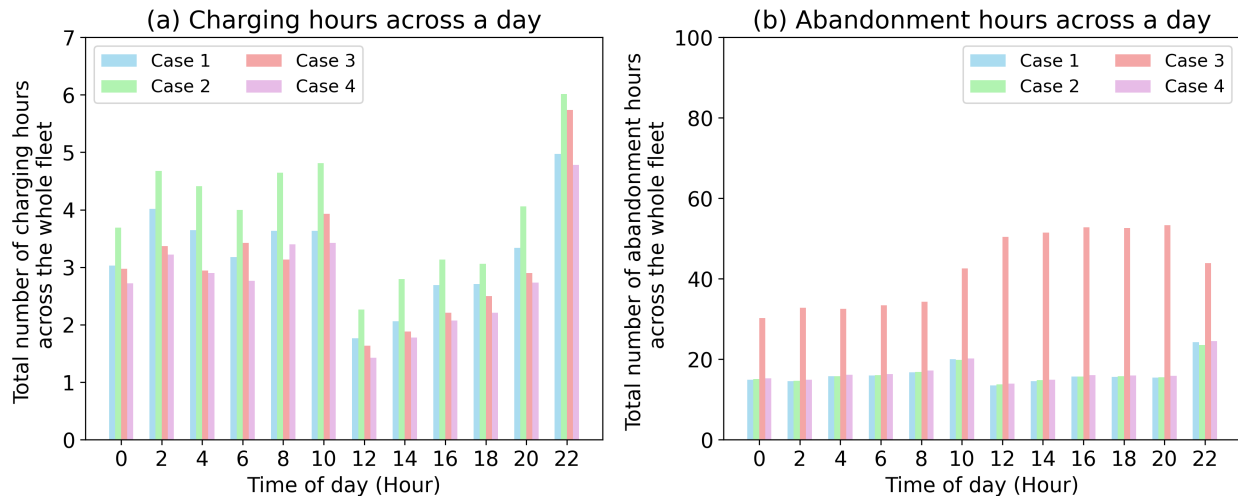


Figure 12 The total number of (a) charging hours and (b) abandonment hours of the truck fleet in different hours of a day in four deterministic cases

truck fleet in different hours of a day in four cases, respectively. Across four instances, the lowest number of charging hours appears at 12:00, and the highest number of charging hours appears at 22:00. If the model does not assign two special zones for overnight charging, the number of abandonment hours will increase by more than a factor of 2.

Fig. 13 (a) illustrates the average SoC of all trucks over 39 days, ranked from the highest to lowest, and Fig. 13 (b) presents the overall battery SoC (maximum, minimum, and average) of the entire fleet in four cases. Among four cases, case 4 (no range anxiety) yields the lowest average SoC (28.4%), whereas case 2 with full parking duration achieves the highest average SoC (45.3%).

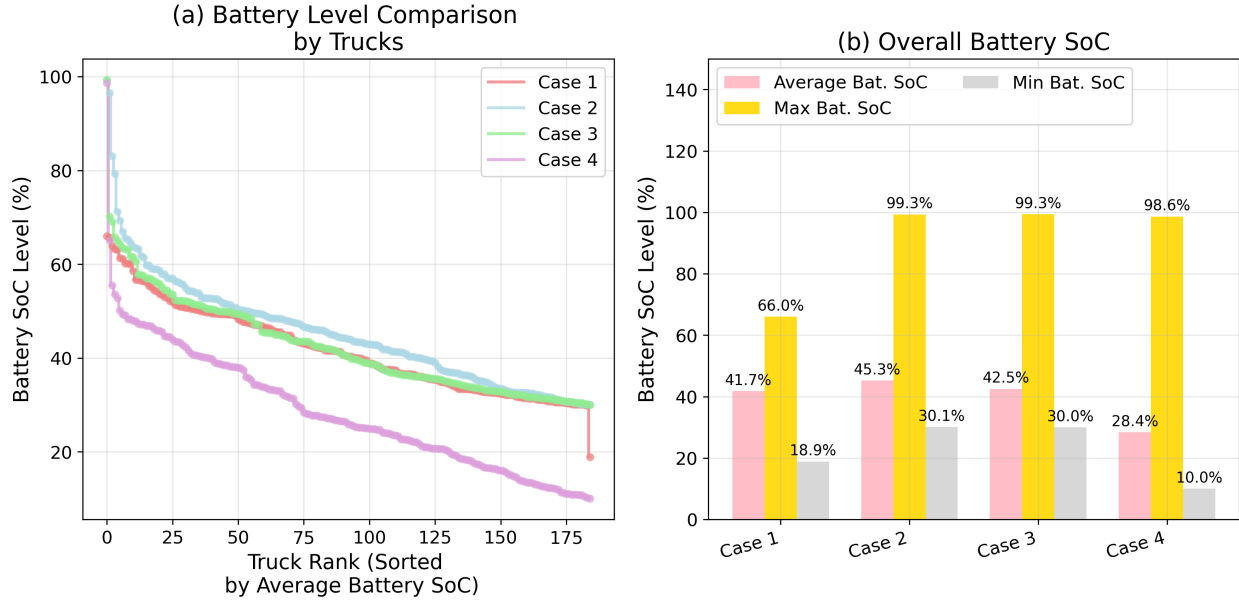


Figure 13 (a) Average SoC of each truck and (b) the overall battery SoC for the entire fleet in four deterministic cases

When the effective charging time constraint is applied, in other words, comparing case 2 to case 1 benchmark, part of the fleet experiences a sharp drop in the average SoC to very low levels ($\leq 20\%$), due to the limited charging duration in the parking windows.

5.5.2. Robust infrastructure planning based on the whole year dataset We then conducted the robust infrastructure planning using the whole year dataset, considering uncertain parking duration. First, we constructed a box-shaped robust uncertainty set using the mean and standard deviation of parking durations, categorized by trucks, hour of a day, and charging zones. We generated four instances by varying the bounds of uncertainty sets, corresponding to 0, 1σ , and 2σ . For the first three instances, we assume that the choice of charging type (slow vs. fast) does not affect the uncertainty of effective parking duration (i.e., $\gamma = 1$). In the fourth instance, however, we assume that fast charging reduces this uncertainty by a factor of two (i.e., $\gamma = 0.5$).

To ensure robust infrastructure planning throughout the year, we optimize the charging infrastructure using two solving approaches: the DS and IPS methods, as described in Section 3. For the DS method, we selected a 39-day horizon and imposed a maximum time limit of 40,000 seconds to solve each instance, recording the gap whenever the solver failed to converge within this limit. For the IPS method, we set a 6-hour time limit for each monthly instance. In addition, we applied the proposed fix-and-optimize heuristic to the 39-day instance under the DS framework, with the initial master problem aligned with the deterministic benchmark case.

Table 4 summarizes the optimization results of four instances under DS, DS with heuristic (DS-h), and IPS methods. Before the optimization, we filter out the HCVs based on the variance equal

Instances (σ, γ)	Solving methods	# of HCVs	# of slow/fast chargers	Installation costs (\$)	Scheduling penalty (\$)	Gap (%)	Time (h)
(0, 1)	DS	19	68/6	330,000	35,678	9.06	11.1
	DS - h	19	68/6	330,000	35,679	0.07	2.40
	IPS	48	77/5	305,500	33,466	0.09	11.3
(1, 1)	DS	19	68/6	330,000	35,658	9.04	11.1
	DS - h	19	69/6	331,500	36,065	0.05	2.15
	IPS	48	75/7	378,500	33,331	0.05	12.0
(2, 1)	DS	19	68/6	330,000	35,736	9.02	11.1
	DS - h	19	69/6	331,500	35,863	0.05	5.20
	IPS	48	76/8	418,000	33,402	0.05	23.8
(2, 0.5)	DS	19	69/5	293,500	35,931	0.06	7.42
	DS - h	19	68/6	330,000	35,715	0.06	3.29
	IPS	48	74/8	415,000	22,541	0.03	29.8

Table 4 Summary of optimization results across four instances using DS, DS with heuristic (DS-h), and IPS methods. For the IPS method, the reported gap is the optimal gap of the final instance in the iterative planning

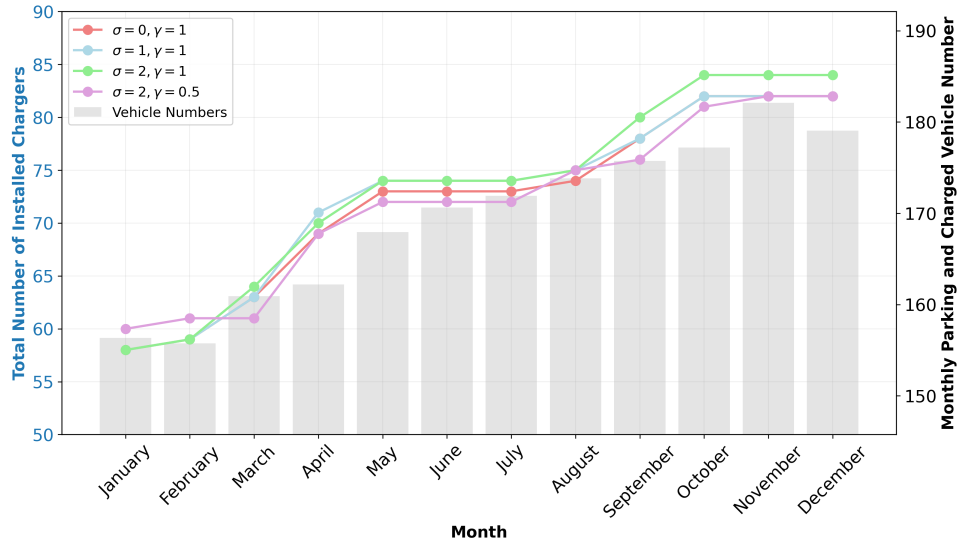


Figure 14 The total number of chargers in each month using the IPS method in four instances (in colored lines) versus the total number of trucks parking and charged (in gray bars) in all eight zones

to 2σ . The DS method yields 19 HCVs in the 39-day dataset, and the IPS method yields 48 HCVs in the whole-year dataset. We find that solving these instances directly with the DS method is difficult to converge, with three out of four cases reaching the maximum time limit. Using the proposed heuristic method, the problem can reach acceptable optimality gaps of less than 0.1% while keeping the computation time within the prescribed limits. It should be noted that we conducted the warm start as the solution of deterministic benchmark case is available, and the time to complete 10 iterations is around 1 hour. Using the IPS method, between one and three instances hit the time limit in the iterative processes. However, all four instances that are solved using the IPS method

converge by the end of the 12-month horizon. For the final instance involving the joint planning and scheduling, an accepted optimality gap of less than 0.1% is achieved.

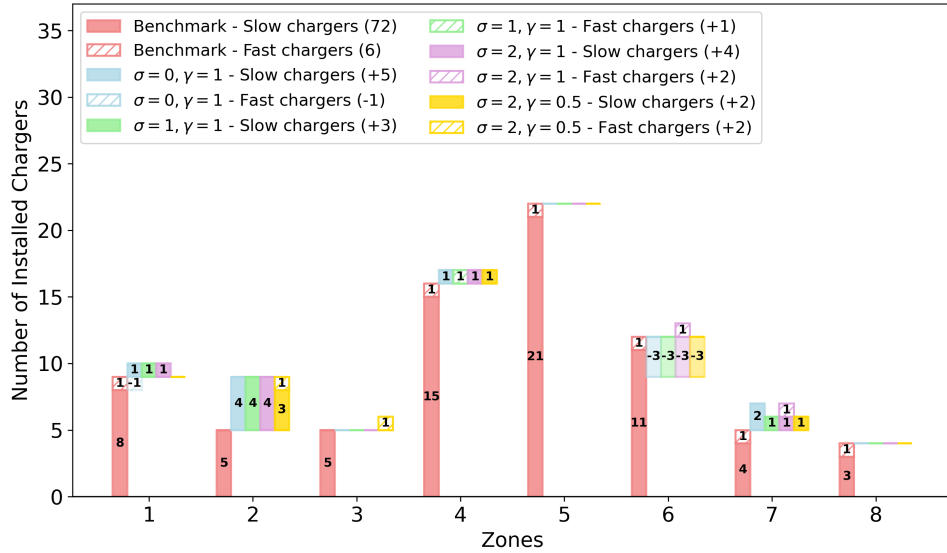


Figure 15 Zone-wise differences in the number of slow and fast chargers in four stochastic cases compared to the benchmark

When comparing the three solution methods, the IPS method yields the highest number of chargers across all four instances using the full-year datasets. The DS and DS-h methods have an even lower number of chargers compared with the deterministic benchmark case, since an additional 18 trucks are excluded as HCVs due to the short parking duration. Fig. 14 shows the total number of chargers (i.e., the sum of fast and slow chargers) determined by the IPS procedure from monthly subproblems over 12 months in the four instances. From January to December, the number of trucks parking and charged in any of the eight zones rises from 156 to 182, leading to a steady increase in the required charger installations. As the parking duration uncertainty grows, the total number of EV chargers—particularly fast chargers—also increases. In the fourth instance, a larger share of fast chargers is installed compared to the third instance, since fast chargers are less affected by uncertainty than slow chargers. Across four stochastic instances, the only difference between the DS and DS-h results lies in the installation or placement of a single fast charger. This indicates that the assignment of specific fast chargers can hinder the convergence of the DS method. In contrast, the proposed heuristic prioritizes placing the fast charger, allowing the model to achieve the optimal solution more efficiently. The detailed solution process using the DS-h method is presented in Appendix F.

Fig. 15 shows the zone-wise differences in the number of slow and fast chargers when comparing four stochastic instances to the benchmark case (i.e., case 1 in the deterministic formulation). In

general, zones 1, 2, 4, and 7 have an increase in the number of slow chargers, while zone 6 has a reduction. It is because that zone 6 has a quite high variance in the parking duration. The model optimizes more chargers and schedules more trucks to be charged at zones 1 or 2, which are connected to zone 6, in four stochastic cases.

5.5.3. The impacts of uncertain parking duration To evaluate the impact of uncertain parking duration on the charger planning and scheduling, we first simulated the monthly schedule based on the charger planning results for the case where $\sigma = 2$ and $\gamma = 0$, using the DS-h and IPS methods, respectively. We found that the charging installation obtained from the DS-h method meets the requirements for only six months, where the number of trucks dispatched is less, whereas those obtained from the IPS method satisfy the requirements for all 12 months. This discrepancy arises from the steadily increasing trend of truck parking and charging activities throughout the year, which the day-selection approach fails to capture adequately during peak months.

Instances (σ, γ)	Avg. slow charging hours	Avg. fast charging hours	Avg. abandonment hours	Avg. charging hours (truck per day)	Avg. charging power (kW)
(0, 1)	3757.6	1280.7	20212.9	0.83	8.78
(1, 1)	2166.9	1249.9	20229.9	0.56	12.95
(2, 1)	2126.3	1357.5	20155.1	0.57	12.70
(2, 0.5)	515.1	1033.0	20191.6	0.25	28.59

Table 5 Summary of the average scheduled charging hours, abandonment hours, and charging power in a year across four instances

We then evaluated four stochastic instances using the IPS method by simulating the charging scheduling in 12 months and calculated the average value of the total charging and abandonment hours by month. Fig. 16 shows the box-plots of the total number of slow and fast charging hours by months in four stochastic instances using the IPS method, and Table 5 summarizes the average scheduled charging hours, abandonment hours, and charging power by months. As the uncertainty increases where the standard deviation of the parking duration σ increases from 0 to 2, the fast charger usage rises while the slow charger usage declines, since the shorter parking durations incentivize drivers to rely more on the fast charging. As the fast chargers are more frequently used, the average charging power increases from 8.78 kW when the standard deviation equals 0, to 12.95 kW and 12.70 kW when the standard deviation equals 1 and 2, respectively. The average abandonment hour keeps the same level across four stochastic instances.

For the second and third instances, where the standard deviations are 1 and 2, respectively, the third instance exhibits longer total charging hours and lower charging rates, even though fast-charging hours are greater than in the second instance. This is because the increased uncertainty in

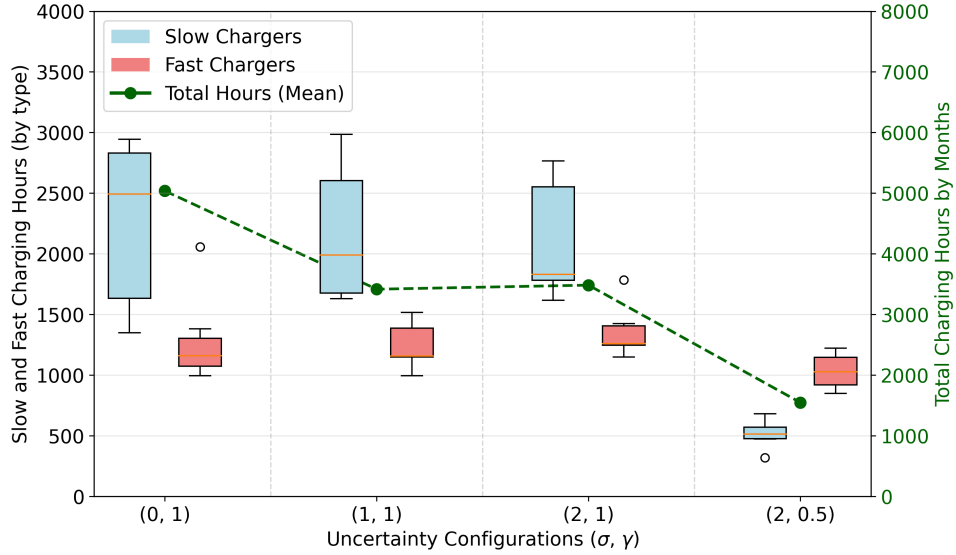


Figure 16 Boxplots of the monthly slow and fast charging hours across four stochastic instances versus the average of charging hours by month

parking duration prolongs overall charging time, offsetting the benefit of more frequent fast charging. In contrast, in the fourth instance—where fast chargers effectively mitigate parking duration uncertainty—the total charging time decreases significantly, with trucks relying on fast chargers for most of the period. The average monthly slow-charging time is only 515.1 hours.

5.6. Conclusion and discussion

We developed a two-stage robust charging infrastructure planning model for the electrification of light-duty trucks at industrial sites with mixed-type chargers with different charging power. The first stage plans the charging infrastructure based on the selected charging locations and charging types. The second stage optimizes the charging schedules considering different waiting times, charging abandonment, and range anxiety. A case study is conducted on an open-pit mining site with eight potential charging zones. We used three input datasets extracted from the whole-year GPS data from around 200 trucks: (i) parking indications at each half-hour interval, (ii) actual parking durations of each parking window, and (iii) half-hour energy consumption of all trucks.

5.6.1. The impacts of overnight charging and range anxiety on charging behaviors

Among eight zones, we assume that two designated zones allow overnight parking; otherwise, trucks will forgo charging if no chargers are available, unless their battery level falls below 30%. The battery SoC status below 30% is assumed to trigger the range anxiety, resulting in an additional half-hour waiting time. The benchmark case based on the selected 39 days yields 72 slow chargers and 6 fast chargers. We then examine three cases where overnight charging, range anxiety, and

limited parking duration in each parking window are not considered, respectively. Extending the parking duration to the full window reduces the number of fast chargers to 3. Removing the designated overnight zones leads to a dramatic increase in abandonment hours by 1.63 times and an additional 20 slow chargers installed in total. No range anxiety requires seven more slow chargers to be installed. In addition, we found that the charging hours only occupy around 4% of the total parking time, meaning the limited waiting time and consequential abandonment are the main reasons that lead to a number of slow chargers at industrial sites.

5.6.2. Robust charging infrastructure planning considering uncertain parking duration To utilize the full-year dataset, we proposed two methods—the DS and IPS approaches—for charging infrastructure planning. The uncertain parking duration within each half-hour parking window is represented using a robust uncertainty set, whose bounds depend on the charging decisions. The IPS method ensures robust scheduling performance throughout the year by planning for a larger number of chargers, whereas the DS method fails in several months when the charging demand peaks.

When the uncertainty of charging duration increases (i.e., the lower bound of the uncertainty set decreases), the total number of fast-charging hours rises, while the total number of slow-charging hours declines. Consequently, the overall average charging power increases under the mixed-type charging infrastructure. However, further reducing the lower bound of the robust set for parking duration to the minimum level (i.e., 5 minutes) leads to longer total charging hours and a decrease in average charging power. If the model incorporates the mitigating effect of fast charging on parking duration uncertainty—observed in many real-world studies—a smaller number of slow chargers would be planned and utilized.

5.6.3. Heuristic methods to assist the robust scheduling with a long optimization horizon The proposed two-stage planning and scheduling framework is formulated as a large-scale MILP model. For a 39-day scheduling instance with 189 trucks, the model contains over 1.5 million binary variables without pre-solving, making it computationally challenging. To address this, we introduce a fix-and-optimize heuristic for the charging scheduling under uncertainty. This is to forecast the high charging demand due to reduced parking duration and to pre-assign fast charging actions in the scheduling. This reduces the computation time by approximately 2-5 times for 39-day instances and yields the optimality gap of the problem below 0.1%.

Finally, several promising avenues remain for future research. For example, future work could incorporate additional charging options, such as multiple types of fast chargers with rated powers exceeding 150 kW, to further reduce the number of required HCVs. Moreover, charging behavior modeling could be improved by integrating empirical data from existing electrified fleets to account for factors like variations in range anxiety at different times of day.

5.7. Acknowledgment

We gratefully acknowledge the sponsor company for providing GPS data from the operating trucks at the mining site. We also thank Maria Isabel Castrillo Viguera for her valuable contributions in processing the GPS data and preparing the input datasets.

References

Abdelwahed, A., Van Den Berg, P. L., Brandt, T., Collins, J., & Ketter, W. (2020, November). Evaluating and Optimizing Opportunity Fast-Charging Schedules in Transit Battery Electric Bus Networks. *Transportation Science*, 54(6), 1601–1615. Retrieved 2025-08-23, from <https://pubsonline.informs.org/doi/10.1287/trsc.2020.0982> doi: 10.1287/trsc.2020.0982

Arena, G., Chub, A., Lukianov, M., Strzelecki, R., Vinnikov, D., & De Carne, G. (2024). A Comprehensive Review on DC Fast Charging Stations for Electric Vehicles: Standards, Power Conversion Technologies, Architectures, Energy Management, and Cybersecurity. *IEEE Open Journal of Power Electronics*, 5, 1573–1611. Retrieved 2025-09-19, from <https://ieeexplore.ieee.org/document/10691639/> doi: 10.1109/OJPEL.2024.3466936

Bertsimas, D., & Hertog, D. d. (2022). *Robust and adaptive optimization*. Belmont, Massachusetts: Dynamic Ideas LLC. (OCLC: 1334655371)

Chen, G., Gayon, J.-P., & Lemaire, P. (2023, September). Technical Note—Stochastic Scheduling with Abandonment: Necessary and Sufficient Conditions for the Optimality of a Strict Priority Policy. *Operations Research*, 71(5), 1789–1793. Retrieved 2025-08-24, from <https://pubsonline.informs.org/doi/10.1287/opre.2022.2285> doi: 10.1287/opre.2022.2285

Chen, L., He, L., & Zhou, Y. H. (2024, September). An Exponential Cone Programming Approach for Managing Electric Vehicle Charging. *Operations Research*, 72(5), 2215–2240. Retrieved 2025-08-24, from <https://pubsonline.informs.org/doi/10.1287/opre.2023.2460> doi: 10.1287/opre.2023.2460

Chen, Y., & Liu, Y. (2023, January). Integrated Optimization of Planning and Operations for Shared Autonomous Electric Vehicle Systems. *Transportation Science*, 57(1), 106–134. Retrieved 2025-08-23, from <https://pubsonline.informs.org/doi/10.1287/trsc.2022.1156> doi: 10.1287/trsc.2022.1156

Cui, D., Wang, Z., Liu, P., Wang, S., Zhao, Y., & Zhan, W. (2023, April). Stacking regression technology with event profile for electric vehicle fast charging behavior prediction. *Applied Energy*, 336, 120798. Retrieved 2025-08-24, from <https://linkinghub.elsevier.com/retrieve/pii/S0306261923001629> doi: 10.1016/j.apenergy.2023.120798

Delarue, A., Lian, Z., & Martin, S. (2025). *Algorithmic Precision and Human Decision: A Study of Interactive Optimization for School Schedules*. Retrieved 2025-01-10, from https://papers.ssrn.com/sol3/papers.cfm?abstract_id=4324076

Fonseca, G. H., Figueiroa, G. B., & Toffolo, T. A. (2024, March). A fix-and-optimize heuristic for the Unrelated Parallel Machine Scheduling Problem. *Computers & Operations Research*, 163, 106504. Retrieved 2025-10-06, from <https://linkinghub.elsevier.com/retrieve/pii/S0305054823003684> doi: 10.1016/j.cor.2023.106504

Ford. (2025, August). *Ford Charge Station Pro*. Retrieved 2025-08-24, from <https://chargers.ford.com/ford-charge-station-pro>

Gkiotsalitis, K., Rizopoulos, D., Merakou, M., Iliopoulou, C., Liu, T., & Cats, O. (2025, March). Electric bus charging station location selection problem with slow and fast charging. *Applied Energy*, 382, 125242. Retrieved 2025-08-23, from <https://linkinghub.elsevier.com/retrieve/pii/S0306261924026266> doi: 10.1016/j.apenergy.2024.125242

Goodall, N. J., & Robartes, E. (2024, January). Feasibility of Battery Electric Pickup Trucks in a State Department of Transportation Fleet. *Transportation Research Record: Journal of the Transportation Research Board*, 2678(1), 760–769. Retrieved 2024-12-20, from <https://journals.sagepub.com/doi/10.1177/03611981231172501> doi: 10.1177/03611981231172501

Hu, H., Du, B., Liu, W., & Perez, P. (2022, August). A joint optimisation model for charger locating and electric bus charging scheduling considering opportunity fast charging and uncertainties. *Transportation Research Part C: Emerging Technologies*, 141, 103732. Retrieved 2025-08-23, from <https://linkinghub.elsevier.com/retrieve/pii/S0968090X2200167X> doi: 10.1016/j.trc.2022.103732

Legault, R., Cabral, F., & Sun, X. A. (2025, July). *Integrated Bus Fleet Electrification Planning Through Accelerated Logic-Based Benders Decomposition and Restriction Heuristics*. doi: <https://doi.org/10.48550/arXiv.2508.05863>

Li, S., Ouyang, W., Ma, Y., & Wu, C. (2025, February). *Learning-Guided Rolling Horizon Optimization for Long-Horizon Flexible Job-Shop Scheduling*. arXiv. Retrieved 2025-10-10, from <http://arxiv.org/abs/2502.15791> (arXiv:2502.15791 [math]) doi: 10.48550/arXiv.2502.15791

Lim, M. K., Mak, H.-Y., & Rong, Y. (2015, February). Toward Mass Adoption of Electric Vehicles: Impact of the Range and Resale Anxieties. *Manufacturing & Service Operations Management*, 17(1), 101–119. Retrieved 2025-08-22, from <https://pubsonline.informs.org/doi/10.1287/msom.2014.0504> doi: 10.1287/msom.2014.0504

Lu, C.-F., Liu, G.-P., Yu, Y., & Cui, J. (2025, April). A Coordinated Model Predictive Control-Based Approach for Vehicle-to-Grid Scheduling Considering Range Anxiety and Battery Degradation. *IEEE Transactions on Transportation Electrification*, 11(2), 5688–5699. Retrieved 2025-08-22, from <https://ieeexplore.ieee.org/document/10739340/> doi: 10.1109/TTE.2024.3488075

Mak, H.-Y., Rong, Y., & Shen, Z.-J. M. (2013, July). Infrastructure Planning for Electric Vehicles with Battery Swapping. *Management Science*, 59(7), 1557–1575. Retrieved 2025-08-22, from <https://pubsonline.informs.org/doi/10.1287/mnsc.1120.1672> doi: 10.1287/mnsc.1120.1672

Mussa, A. S., Klett, M., Behm, M., Lindbergh, G., & Lindström, R. W. (2017, October). Fast-charging to a partial state of charge in lithium-ion batteries: A comparative ageing study. *Journal of Energy Storage*, 13, 325–333. Retrieved 2025-08-23, from <https://linkinghub.elsevier.com/retrieve/pii/S2352152X17301913> doi: 10.1016/j.est.2017.07.004

Nohadani, O., & Sharma, K. (2018, January). Optimization under Decision-Dependent Uncertainty. *SIAM Journal on Optimization*, 28(2), 1773–1795. Retrieved 2025-08-24, from <https://pubs.siam.org/doi/10.1137/17M1110560> doi: 10.1137/17M1110560

Noyan, N., Rudolf, G., & Lejeune, M. (2022, March). Distributionally Robust Optimization Under a Decision-Dependent Ambiguity Set with Applications to Machine Scheduling and Humanitarian Logistics. *INFORMS Journal on Computing*, 34(2), 729–751. Retrieved 2025-09-14, from <https://pubsonline.informs.org/doi/10.1287/ijoc.2021.1096> doi: 10.1287/ijoc.2021.1096

Primecomtech. (n.d.). *Primecom.Tech Level 3DC Dual Dispenser EV Supercharger DC Fast Charger for Electric Vehicle.* Retrieved 2025-08-24, from https://www.primecom.tech/products/primecom-tech-level-3-dc-dual-dispenser-charging-ev-supercharger-fast-charger-for-electric-vehicles?currency=USD&variant=49975633805629&utm_source=google&utm_medium=cpc&utm_campaign=Google%20Shopping&stkn=aa93a15a64b1&srsltid=AfmB0orf7Dr90QMKCb4Ias0yhgnqBb36AuL10XIKudfjaNDXbNviPSm6uI

Sevdari, K., Calearo, L., Bakken, B. H., Andersen, P. B., & Marinelli, M. (2023, December). Experimental validation of onboard electric vehicle chargers to improve the efficiency of smart charging operation. *Sustainable Energy Technologies and Assessments*, 60, 103512. Retrieved 2025-09-19, from <https://linkinghub.elsevier.com/retrieve/pii/S2213138823005052> doi: 10.1016/j.seta.2023.103512

Staffell, I., & Pfenninger, S. (2016, November). Using bias-corrected reanalysis to simulate current and future wind power output. *Energy*, 114, 1224–1239. Retrieved 2025-08-23, from <https://linkinghub.elsevier.com/retrieve/pii/S0360544216311811> doi: 10.1016/j.energy.2016.08.068

Tao, Y., Qiu, J., Lai, S., Wang, G., Liu, H., & Sun, X. (2024, July). Coordinated Planning of Dynamic Wireless Charging Systems and Electricity Networks Considering Range Anxiety of Electric Vehicles. *IEEE Transactions on Smart Grid*, 15(4), 3876–3891. Retrieved 2025-08-23, from <https://ieeexplore.ieee.org/document/10402092/> doi: 10.1109/TSG.2024.3355183

US Department of Transportation. (2025, January). *Charger Types and Speeds.* Retrieved 2025-08-30, from <https://www.transportation.gov/rural/ev/toolkit/ev-basics/charging-speeds>

U.S. EPA. (2024, May). *Facts U.S. Transportation Sector Greenhouse Gas Emissions 1990 –2022* (Tech. Rep.). U.S. EPA. Retrieved 2025-09-14, from <https://nepis.epa.gov/Exe/ZyPDF.cgi?Dockey=P101AKR0.pdf>

Zhang, Y., Li, S., Blythe, P., Wardle, J., Herron, C., Edwards, S., ... Namdeo, A. (2025, March). Analysis of electric vehicle charging behaviour in existing regional public and workplace charging infrastructure: A case study in the North-East UK. *Transportation Engineering*, 19, 100309. Retrieved 2025-08-24,

from <https://linkinghub.elsevier.com/retrieve/pii/S2666691X25000090> doi: 10.1016/j.treng.2025.100309

Appendix A: Waiting time and abandonment: full illustrations

State evolution on a parked stretch. Recall that $S_{i,d,t} \in \{0, 1\}$ indicate that (i, d, t) is a parking slot and $z(i, d, t)$ be the zone index when $S_{i,d,t} = 1$. Define the *continuity indicator*

$$\kappa_{i,d,t} := \begin{cases} 1, & S_{i,d,t} = 1, S_{i,\tilde{d},\tilde{t}} = 1, z(i, d, t) = z(i, \tilde{d}, \tilde{t}), \\ 0, & \text{otherwise,} \end{cases}$$

where (\tilde{d}, \tilde{t}) is the previous admissible slot (day wrap as needed). Then the implemented rules are equivalently

$$w_{i,d,t} = \begin{cases} 0, & S_{i,d,t} = 0 \text{ or } \kappa_{i,d,t} = 0, \\ w_{i,\tilde{d},\tilde{t}} + \Delta t \left(1 - \sum_{j \in \mathcal{J}} y_{i,\tilde{d},\tilde{t}}^j \right), & \text{otherwise,} \end{cases} \quad a_{i,d',t'} \geq a_{i,d,t} \text{ for the next slot } (d', t').$$

Hence: (i) any charge in (\tilde{d}, \tilde{t}) prevents growth of w in that step; (ii) any zone change resets w ; (iii) day-to-day carryover is allowed only when the zone is unchanged.

Worked example 1 (day boundary, same zone). Consider three consecutive admissible slots for truck i in the same zone: $(d, t=1)$, $(d, t=2)$, and $(d+1, 0)$, none charged. Then $w_{i,d,1} = 0$, $w_{i,d,2} = \Delta t$, and $w_{i,d+1,0} = 2\Delta t$, matching Fig. 2.

Worked example 2 (zone switch). Let $(d, 1)$ and $(d, 2)$ be in Zone 1 and $(d, 3)$ in Zone 2. If no charging occurs, $w_{i,d,1} = 0$, $w_{i,d,2} = \Delta t$, but $w_{i,d,3} = 0$ because the zone changed, as in Fig. 3.

Range anxiety and special zones. In non-special zones, the cap $T_{i,d,t}^{\max} = \Delta t \cdot \delta_{i,d,t}^{30}$ implies: (a) if $\text{SoC} \geq 30\%$, then $\delta_{i,d,t}^{30} = 0$ and the cap is 0; the truck either charges immediately or abandons; (b) if $\text{SoC} < 30\%$, then one slot of waiting is permitted before abandonment. In special (overnight) zones, $T_{i,d,t}^{\max} = L$ so multi-slot waiting is admissible and w can grow across the night until charging starts.

Two operational variants. We support two abandonment policies that only affect when resets are triggered:

1. **Current-policy variant.** Resets occur only on parking gaps or zone changes. If the next slot is admissible and in the same zone, apply (6) and $a_{i,d',t'} \geq a_{i,d,t}$.
2. **SoC-based variant.** In addition to the above, designated *special* slots (e.g., transition markers tied to SoC rules or overnight delineations) force a reset: if (i, d, t) is special, set $w_{i,d,t} = 0$ and do not apply carryover from (6) to the next slot.

Consistency with effective charging time. Within each parked slot, the available charging time is the *effective duration* $\hat{p}_{i,d,t} \in [5/30, 1]$. Charging power is bounded by

$$p_{i,d,t}^{\text{ch}} \leq \sum_{j \in \mathcal{J}} \eta_j P_j \Delta t y_{i,d,t}^j \hat{p}_{i,d,t},$$

so even when w grows across a long stretch (e.g., in a special zone), the energy deliverable in any individual slot remains limited by $\hat{p}_{i,d,t}$.

Appendix B: The value range of M in the Big-M constraints

We specify data-driven, *minimal sufficient* values for the Big-M constants used in (3), (8), and (17)–(18). Throughout, the SoC bounds are those already imposed in the model, $SoC^{\min} \leq b_{i,d,t} \leq SoC^{\max}$.

Low-SoC indicator (M_1) in (3). Constraint (3) encodes the threshold at 30% with a small $\epsilon > 0$. To make (3) logically equivalent to the intended rule $\delta_{i,d,t}^{30} = 1 \Leftrightarrow b_{i,d,t} \leq 0.3$ and $\delta_{i,d,t}^{30} = 0 \Leftrightarrow b_{i,d,t} \geq 0.3 + \epsilon$, it suffices to take

$$M_1^* = \max\{SoC^{\max} - 0.3, 0.3 + \epsilon - SoC^{\min}\}.$$

Waiting-time cap with abandonment (M_2) in (8). Write $T_{i,d,t}^{\max}$ as in (9). Within non-special zones, the worst-case feasible waiting time over any contiguous admissible segment $I \subseteq S_{i,d}^{NZ}$ is exactly its duration $|I|\Delta t$. Define

$$W_{\max} := \max_{i,d} \max_{\text{contiguous } I \subseteq S_{i,d}^{NZ}} (|I|\Delta t).$$

Then taking $M_2^* = W_{\max}$ makes (8) nonbinding whenever $a_{i,d,t} = 1$; when $a_{i,d,t} = 0$, it reduces to the intended cap $w_{i,d,t} \leq T_{i,d,t}^{\max}$. If $M_2 < W_{\max}$, feasibility would be cut off, so M_2^* is minimal.

Fast-charging SoC ceiling (M_3) in (17)–(18). For the constraints $b_{i,d,t} \leq 0.8 + M_3(1 - y_{i,d,t,1})$ and $b_{i,d',t'} \leq 0.8 + M_3(1 - y_{i,d,t,1})$, we require that when the fast charger is *not* used ($y_{i,d,t,1} = 0$) the right-hand side be at least SoC^{\max} . Thus the minimal sufficient choice is

$$M_3^* = SoC^{\max} - 0.8.$$

Computation of W_{\max} and W_{\max}^Z . The longest feasible waiting time in each zone type is the duration of the longest contiguous parked stretch. Hence we compute

$$W_{\max} = \max_{i,d} \max_{\text{contiguous } I \subseteq S_{i,d}^{NZ}} (|I|\Delta t), \quad W_{\max}^Z = \max_{i,d} \max_{\text{contiguous } I \subseteq S_{i,d}^Z} (|I|\Delta t).$$

Summary.

$$M_1^* = \max\{SoC^{\max} - 0.3, 0.3 + \epsilon - SoC^{\min}\},$$

$$M_2^* = W_{\max}, \quad L^* = W_{\max}^Z,$$

$$M_3^* = SoC^{\max} - 0.8.$$

In implementation, set ϵ on the order of the solver feasibility tolerance (e.g., 10^{-6} – 10^{-4}) and, if desired, add a small margin of the same order to each M^* . When indicator constraints are available, these Big-M forms may be replaced by indicator constraints to improve relaxation strength; we keep the Big-M form for consistency.

Appendix C: The addition proof for linearizing the decision-dependent uncertainty set

Assuming that the charging power is restricted by the lower bound, which is set to be the mean minus one standard deviation,

$$p_{i,d,t}^{ch} \leq \sum_{j \in \mathcal{J}} \eta^j \cdot P^j \cdot \Delta t \cdot y_{i,d,t}^j \cdot (\hat{\mu} \cdot y_{i,d,t}^j - \hat{\sigma} \cdot \gamma^j \cdot y_{i,d,t}^j) \quad \forall i, d, t \in \mathcal{S} \quad (25)$$

The nonlinear part $y_{i,d,t}^j \cdot y_{i,d,t}^j$ can be linearized by introducing the binary variable z .

$$p_{i,d,t}^{ch} \leq \sum_{j \in \mathcal{J}} \eta^j \cdot P^j \cdot \Delta t \cdot (\hat{\mu} \cdot z - \hat{\sigma} \cdot \gamma^j \cdot z), \quad \forall i, d, t \in \mathcal{S} \quad (26)$$

where the following constraints applying to z ,

$$z \leq y_{i,d,t}^j \quad (27)$$

$$z \geq y_{i,d,t}^j + y_{i,d,t}^j - 1 \quad (28)$$

$$z \in \{0, 1\} \quad (29)$$

From the observation, we can obtain,

$$z = y_{i,d,t}^j \quad (30)$$

Finally, we can obtain that,

$$p_{i,d,t}^{ch} \leq \sum_{j \in \mathcal{J}} \eta^j \cdot P^j \cdot \Delta t \cdot (\hat{\mu} \cdot y_{i,d,t}^j - \hat{\sigma} \cdot \gamma^j \cdot y_{i,t,z}^j), \quad \forall i, d, t \in \mathcal{S} \quad (31)$$

Appendix D: Data processing

D.1. Detailed statistics of eight charging zones

We identified eight EV charging zones for trucks using GPS records, which include the latitude, longitude, and speed of the truck at each timestamp. For each truck, the algorithm tracks the movement of trucks by converting GPS coordinates into UTM coordinates and measuring the distance between two consecutive points. Please note that we do not consider the charging of elevation at the mining site. We grid divided the entire mining site into 100 meter \times 100 meter square regions. If the truck moves less than 50 meters for longer than 5 minutes, this square is marked as a potential stop. Each stop point is recorded along with the truck ID, coordinates, and duration of the stop, forming a list of candidate charging locations.

We ranked all the candidate charging locations by the total number of single stops throughout a year and selected the top eight charging zones with the highest number of single stops. Table 6 lists the traffic stop statistics of eight charging zones. Different zones have different parking patterns; for instance, zones 1 and 4 are generally for overnight parking, with the average duration of a single stop longer than 8 hours, while zones 5-8 are for driving through, with the average duration of a single stop less than 4 hours.

Metric	SQ1	SQ2	SQ3	SQ4	SQ5	SQ6	SQ7	SQ8
Number of single stops	28,391	2,542	8,746	84,543	83,455	33,568	13,873	14,686
Relative to total (%)	10.41	0.93	3.21	30.99	30.60	12.31	5.09	5.38
Total time stopped by whole fleet of trucks (in year)	11,675	3,716	1,418	15,258	7,624	2,451	1,305	1,110
Relative to total (%)	25.76	8.20	3.13	33.66	16.82	5.41	2.88	2.45
Average duration of a single stop (hours)	9.9	35.1	3.9	4.3	2.2	1.8	2.3	1.8
# trucks stopping	184	154	44	193	181	164	126	130
Average days stopped in a year (per truck)	63.5	24.1	32.2	79.1	42.1	14.9	10.4	8.5
Average hours stopped in a day (hours per day)	4.2	1.6	2.1	5.2	2.8	1.0	0.7	0.6

Table 6 Traffic stop statistics of eight charging zones (SQ1: Roadhouse, SQ2: Airfield, SQ3: Infrastructure, SQ4: Equipment maintenance, SQ5: Plant crusher, SQ6: West facility, SQ7: North facility, SQ8: East facility)

D.2. Processing the annual dataset based on the DS and IPS methods

For the DS method, 39 representative days are selected based on ten criteria listed in Table 7. We ranked 365 days of all years based on these ten criteria, and the top or bottom indicates the direction in which the top day gets selected. Based on the criteria in Table 7, we selected the 39 days listed in Table 8. To maintain continuity in the truck traveling data, consecutive days adjacent to these top-ranked dates are also included. Additionally, the first and last two days of the year are included to ensure the completeness of the selected dataset.

Table 7 10 criterion for selecting representative days

No.	Criteria Description	Ranking from	First day
1	Total fleet distance	Top	2023-12-14
2	# of moving trucks	Top	2023-12-05
3	Average distance per moving truck	Top	2023-01-07
4	# of individual trucks > 296 km	Top	2023-06-16
5	Total fleet energy consumption (EC)	Top	2023-12-14
6	# of consuming trucks	Top	2023-11-21
7	Average EC per consuming truck	Top	2023-01-07
8	# of individual trucks with EC > 75 kWh	Top	2023-03-05
9	Total stopping hours (whole fleet) in any area	Bottom	2023-12-31
10	# of trucks stopped in any area along the day	Bottom	2023-01-08

D.3. Input data generation

The model requires three inputs extracted from the GPS data (1) parking time window indication matrix to show if the truck is parked at any of eight zones at each half-hour time interval (i.e., 1 means parking and 0 means not parking), (2) actual parking time duration, and (3) energy consumption of each truck. Fig. 17 (a) shows an example of the input datasets for three days, and Fig. 17 (b) summarizes the procedure in the flow chart.

Table 8 The 39-day summary by ten criteria

From	To	Number of days	Criteria
2023-01-01	2023-01-02	2	Initial padding
2023-01-05	2023-01-10	6	criteria 3, 7, 10
2023-03-03	2023-03-07	5	criteria 8
2023-06-14	2023-06-18	5	criteria 4
2023-11-19	2023-11-23	5	criteria 6
2023-12-03	2023-12-07	5	criteria 2
2023-12-12	2023-12-19	8	criteria 1, 5
2023-12-29	2023-12-31	3	criteria 9
total		39	

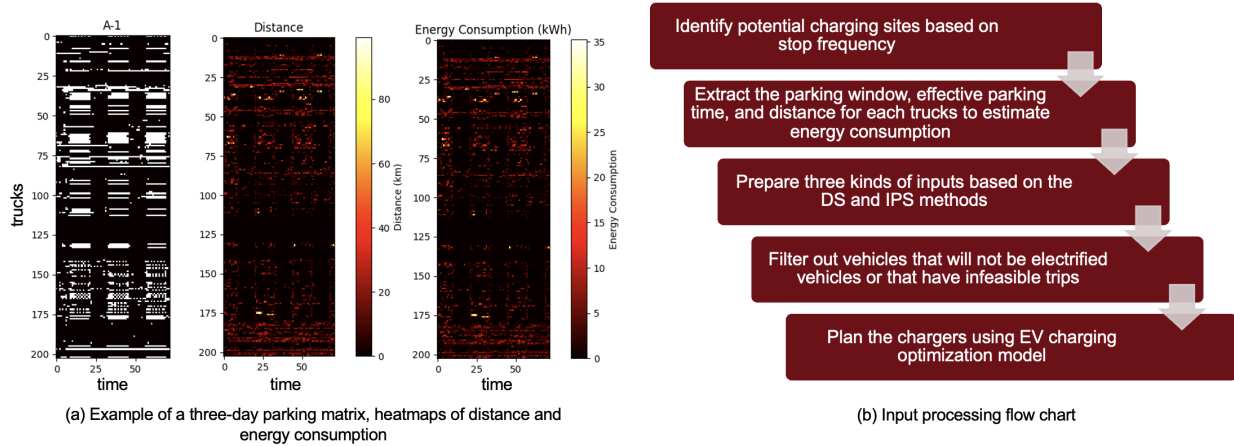


Figure 17 Input data extracted from the GPS data of 203 trucks in three days: parking time window in the charging zone 1, traveling distance, and energy consumption (from right to left); and (b) flow chart for EV charger planning

For the half-hour energy consumption of each truck, we calculated their travel distance (in km) and then converted to energy consumption (kWh) for each half-hour time window, using a second-order, temperature-dependent fuel economy model for U.S. trucks Goodall & Robartes (2024). The hourly temperature data of the mining site is taken from Staffell & Pfenninger (2016). Fig. 18 shows the hourly temperature and the corresponding fuel economy across the year.

Appendix E: Additional results of four deterministic cases

This section presents the detailed optimization result of four deterministic cases: Case 1 (Benchmark), Case 2 (Full parking duration), Case 3 (No special zones), and Case 4 (No range anxiety). Figs. 19, 21, 23, and 25 present the aggregated charging results of eight zones for four cases, and Figs. 20, 22, 24, and 26 present the individual charging results of 188 trucks at eight charging zones.

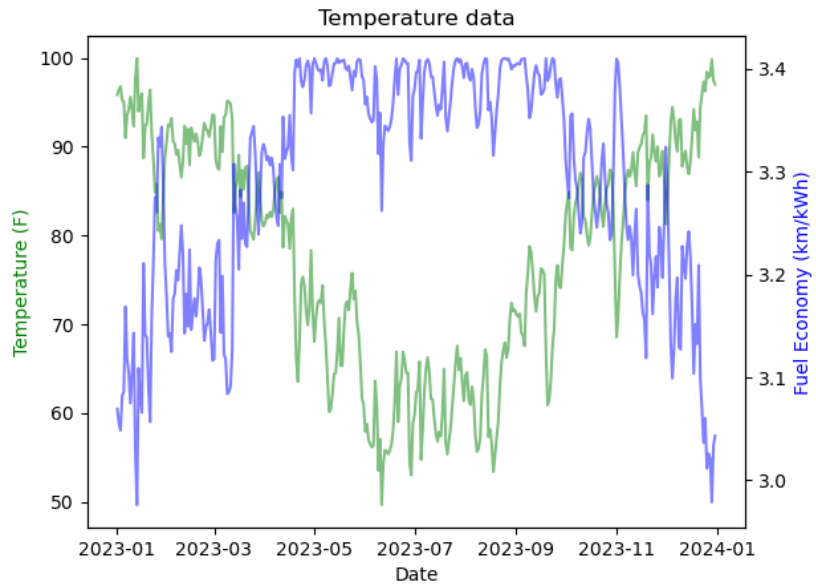


Figure 18 The outdoor temperature (F) and corresponding fuel economy (km/kWh) across the year at the mining site

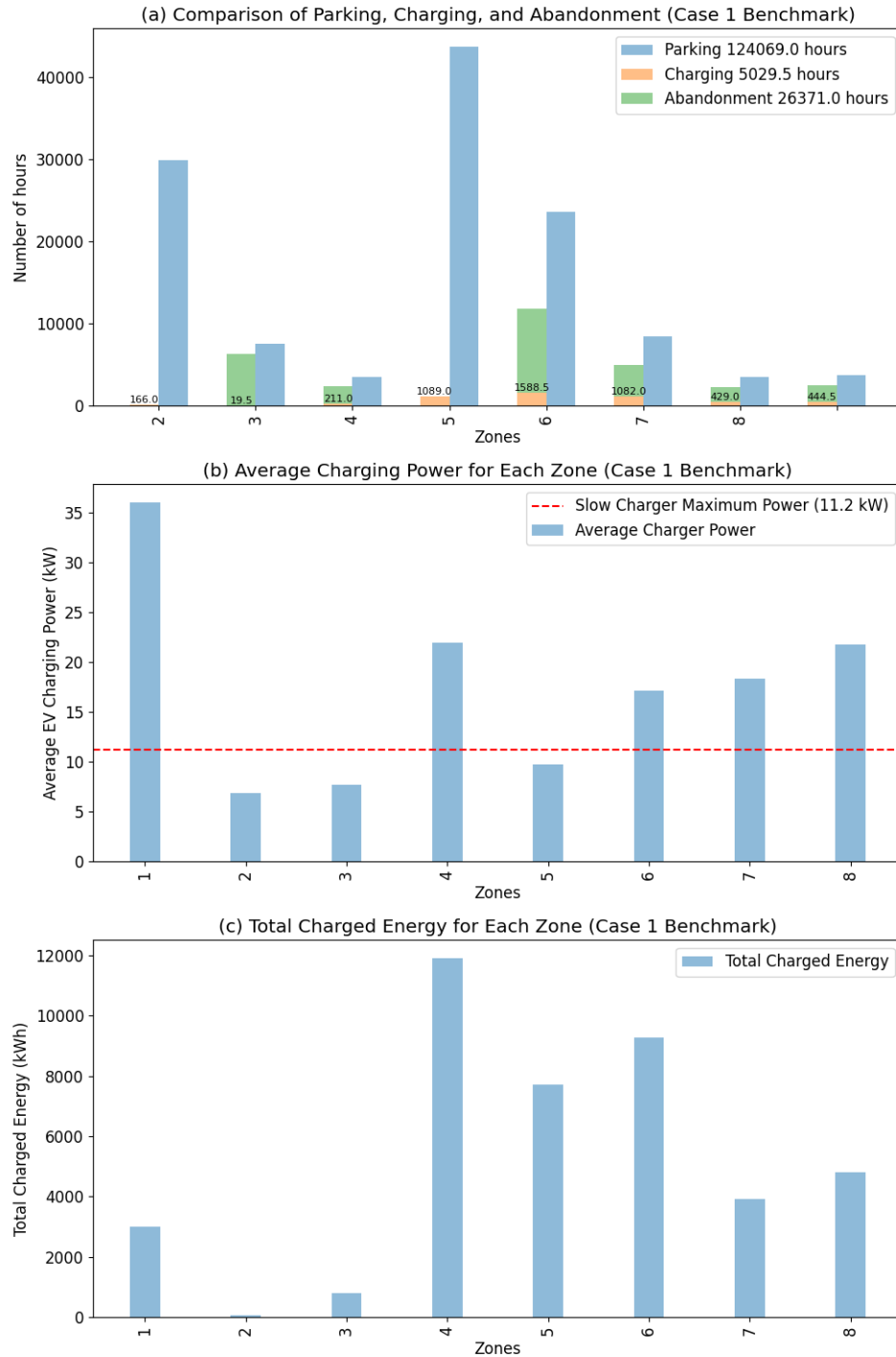


Figure 19 The aggregated charging results of eight zones for case 1 benchmark: (a) The total hours of parking, charging, and abandonment during 39 representative days; (b) The average charging power for each zone during 39 representative days, and (c) the total charged energy for each zone during 39 representative days

Merged Abandonment, Charging, Parking Schedule Across Zones
(Case 1 Benchmark)

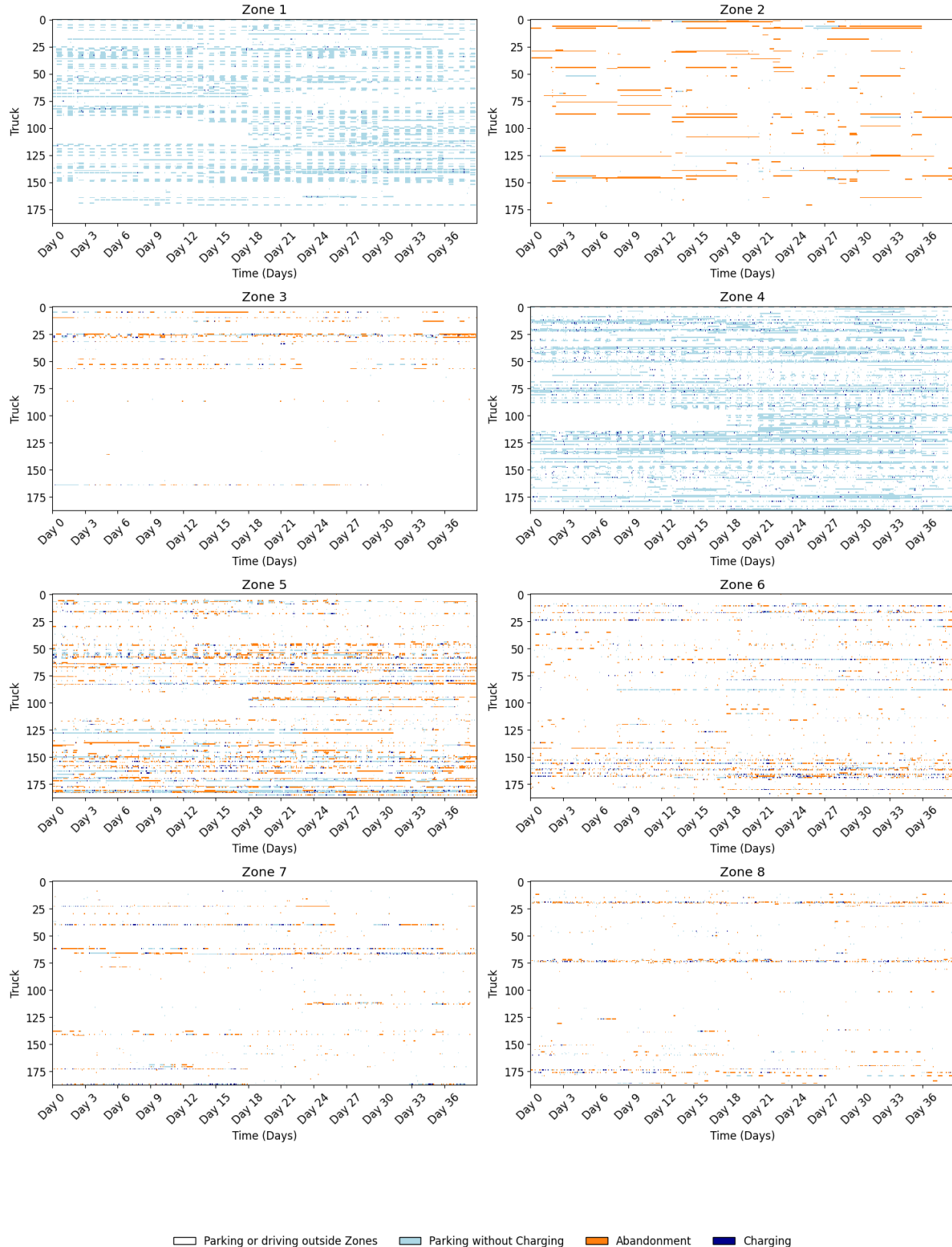


Figure 20 The individual charging schedules of 188 trucks across eight charging zones, arranged from left to right and top to bottom, in the Case 1 benchmark

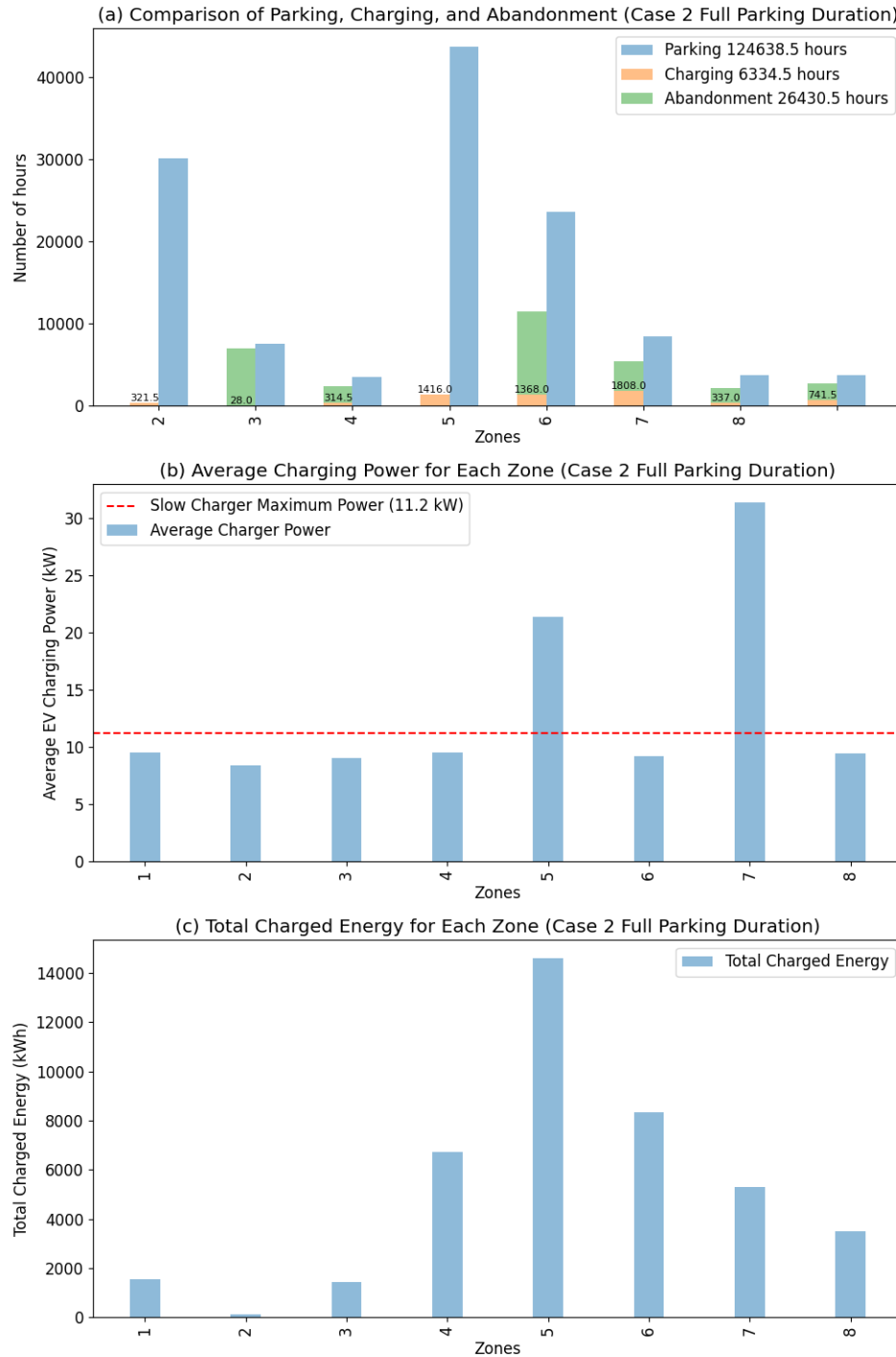


Figure 21 The aggregated charging results of eight zones for case 2 full parking duration: (a) The total hours of parking, charging, and abandonment during 39 representative days; (b) The average charging power for each zone during 39 representative days and (c) the total charged energy for each zone during 39 representative days

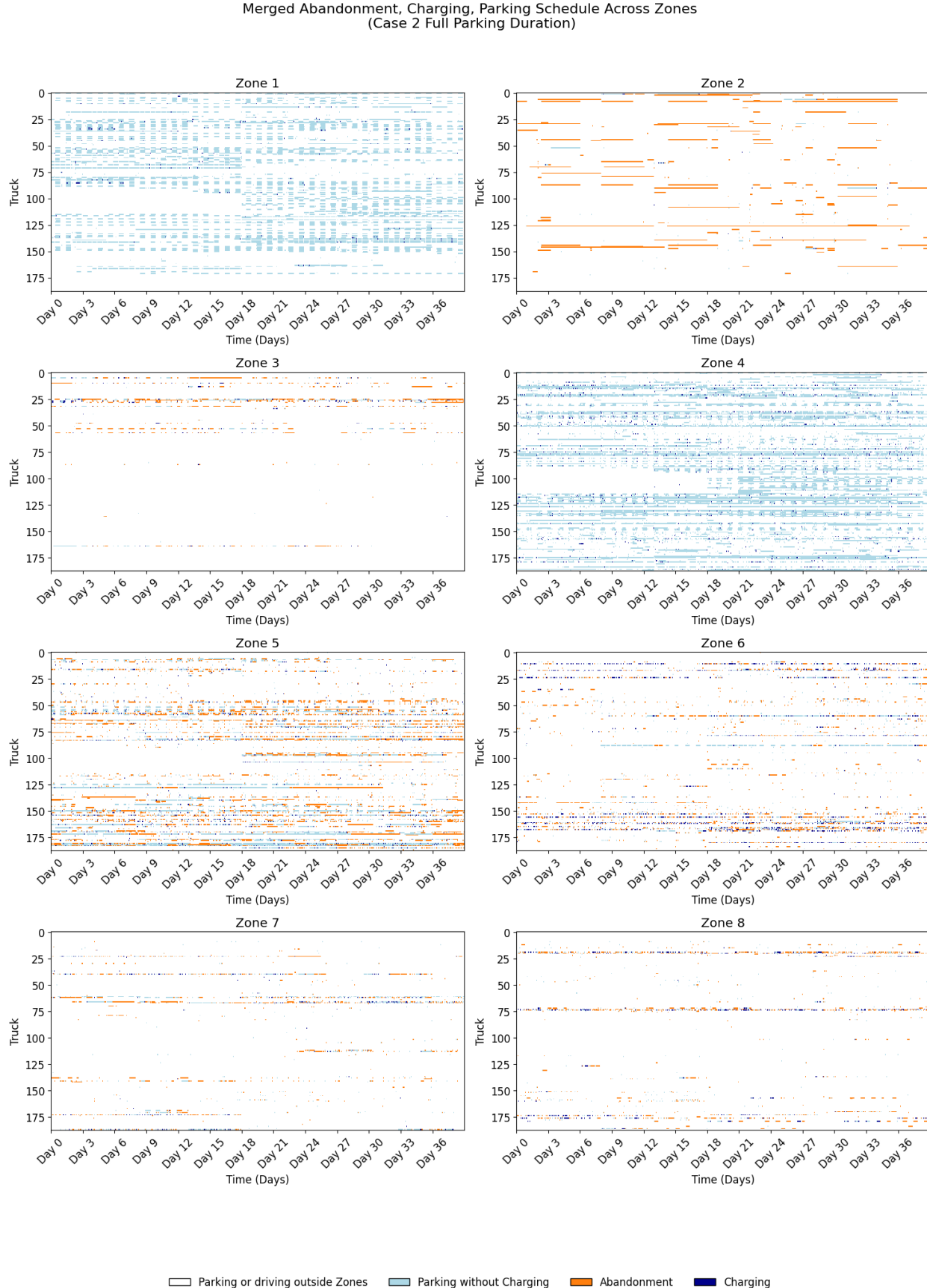


Figure 22 The individual charging scheduling of 188 trucks at eight charging zones, arranged from left to right and top to bottom, in Case 2 full parking duration

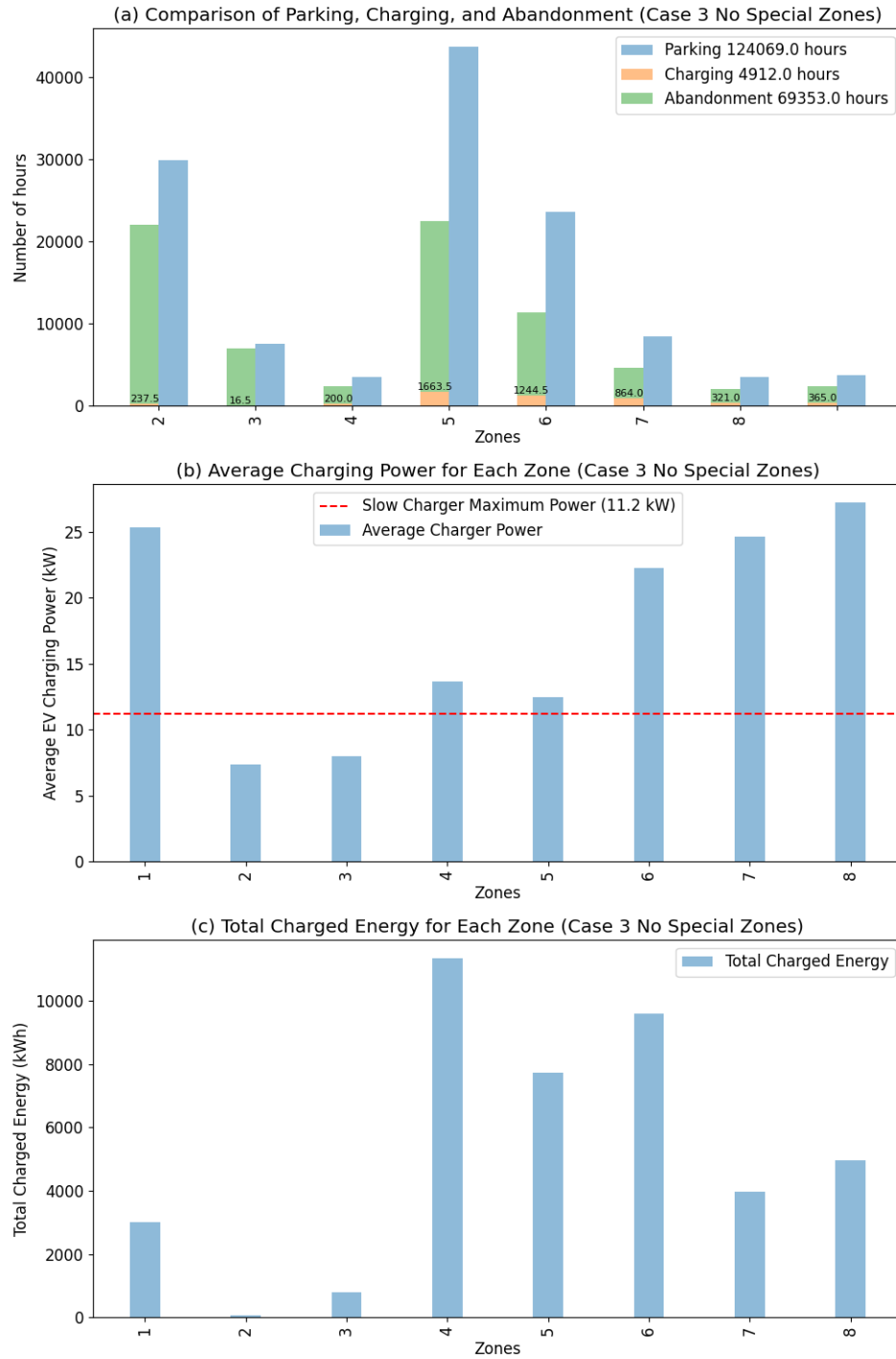


Figure 23 The aggregated charging results of eight zones for case 3 no special zones: (a) The total hours of parking, charging, and abandonment during 39 representative days; (b) The average charging power for each zone during 39 representative days and (c) the total charged energy for each zone during 39 representative days

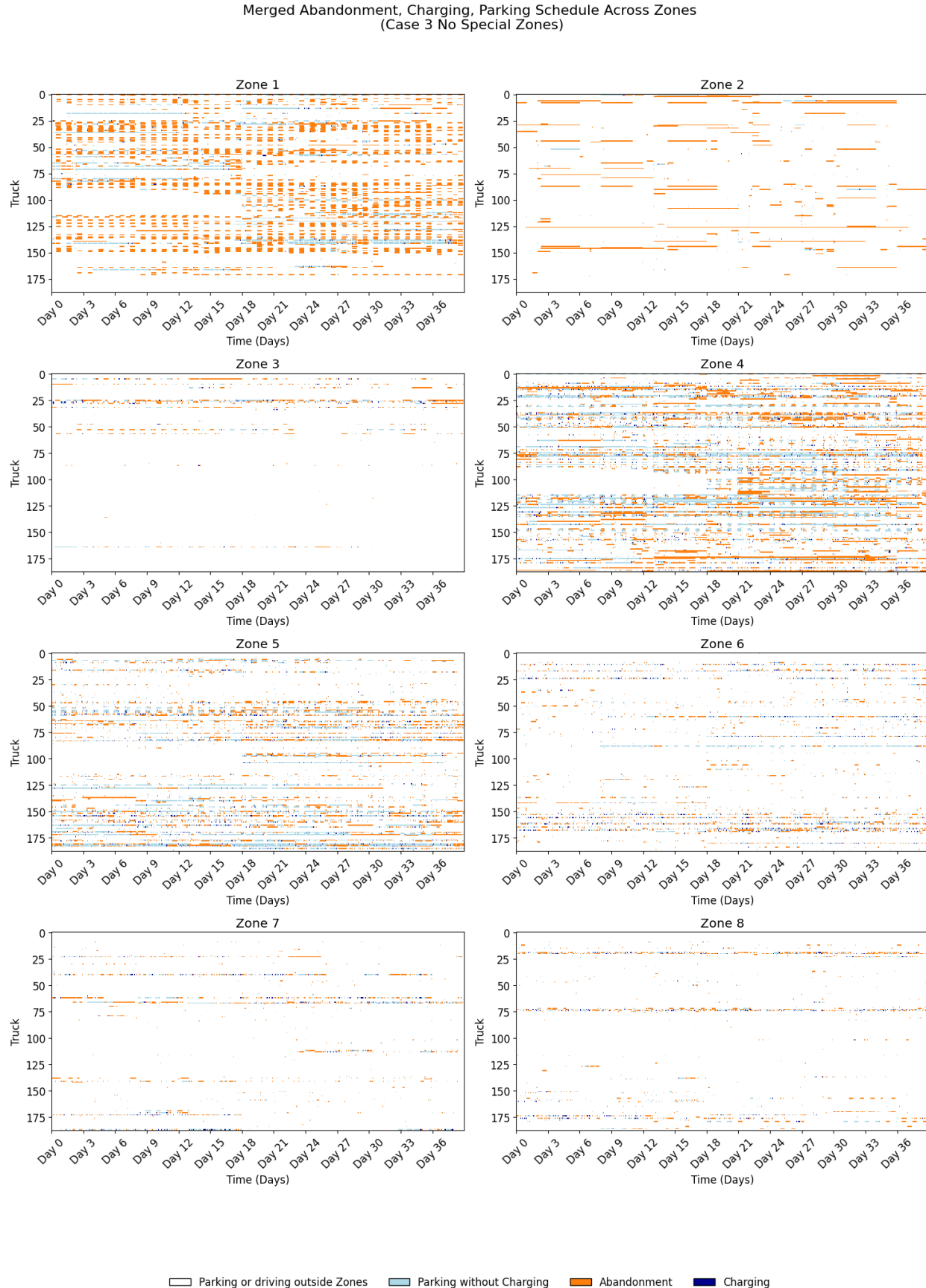


Figure 24 The individual charging scheduling of 188 trucks at eight charging zones, arranged from left to right and top to bottom, in Case 3 no special zones

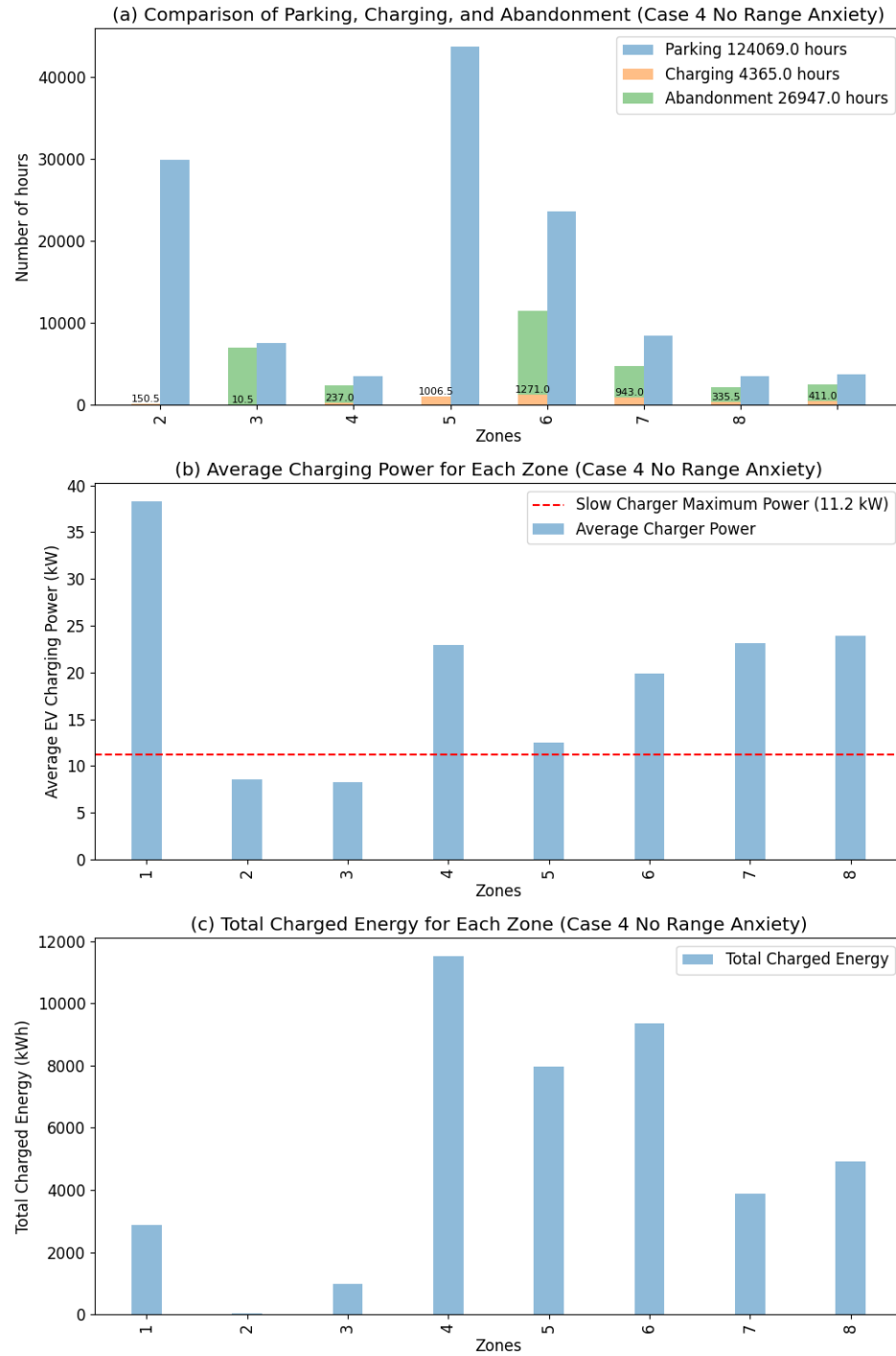


Figure 25 The aggregated charging results of eight zones for case 4 no range anxiety: (a) The total hours of parking, charging, and abandonment of each zone during 39 representative days; (b) The average charging power for each zone during 39 representative days and (c) the total charged energy for each zone during 39 representative days

Merged Abandonment, Charging, Parking Schedule Across Zones
(Case 4 No Range Anxiety)

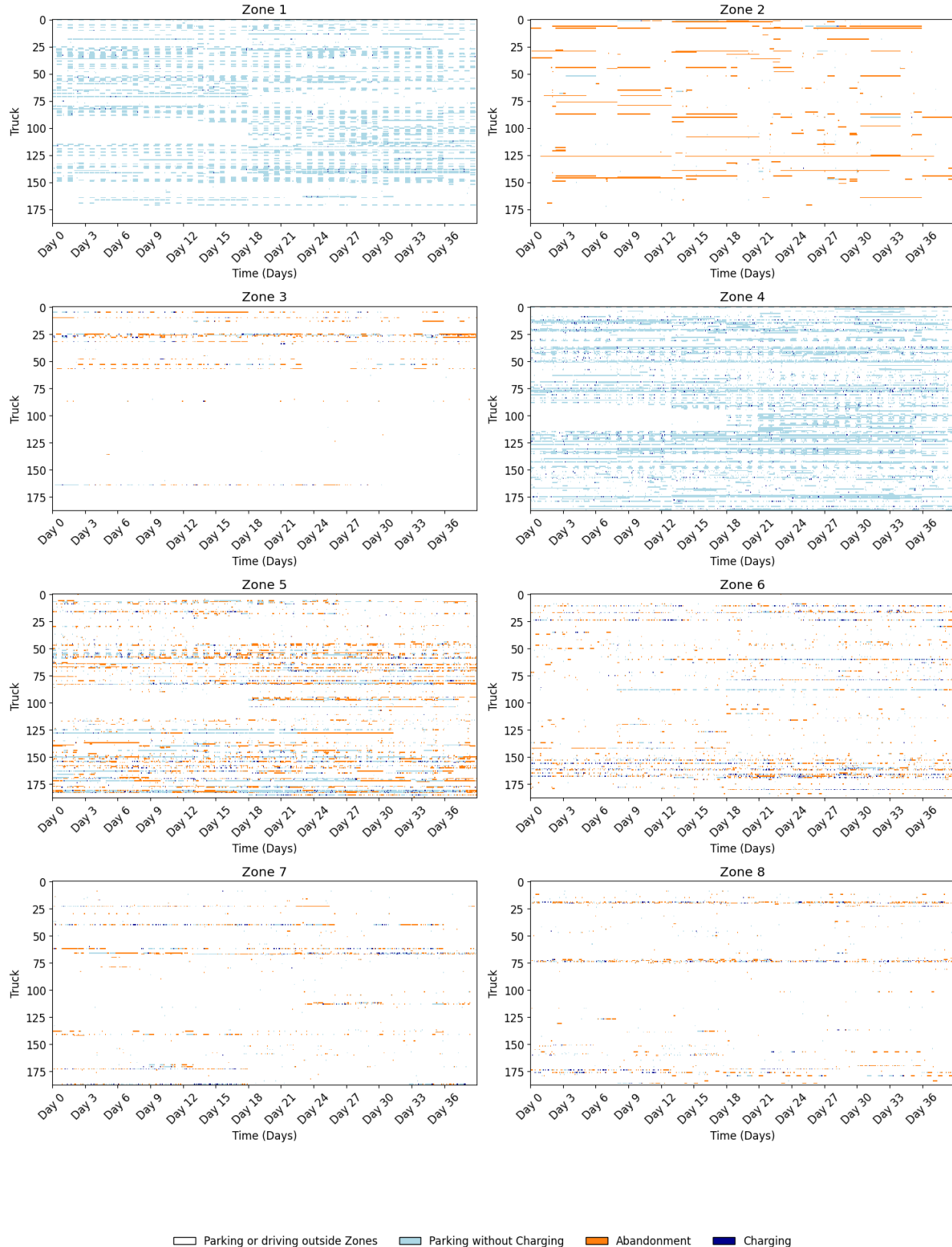


Figure 26 The individual charging scheduling of 188 trucks at eight charging zones, arranged from left to right and top to bottom, in Case 4 no range anxiety

Appendix F: The detailed procedure of the fix-and-optimize algorithm

This section presents the detailed iteration procedures using the fix-and-optimize algorithm. Figs. 27 and 29 present changes of enforced fast-charging constraints and the consequential solving time for the 39-day instance. Figs. 28 and 30 present the evolutions of the number of slow and fast chargers in each iterations.

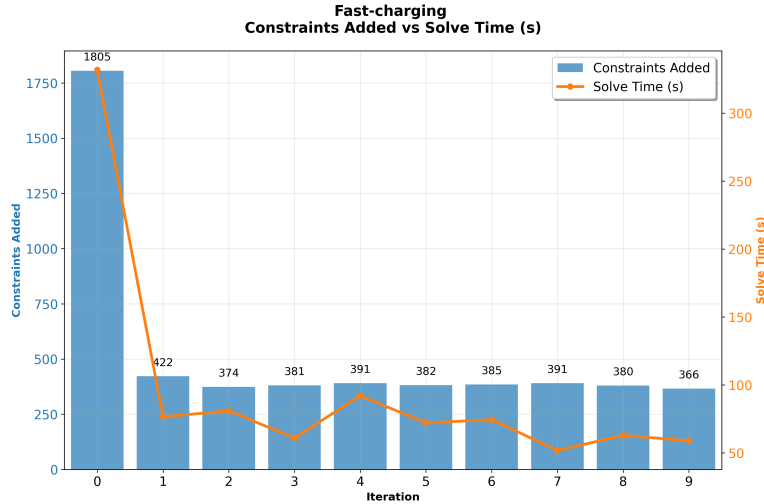


Figure 27 The number of fast-charging constraints incorporated into the scheduling during each iteration and the corresponding solving time for the 39-day instance after applying the constraints with a warm start under the setting $\sigma = 2$ and $\gamma = 1$

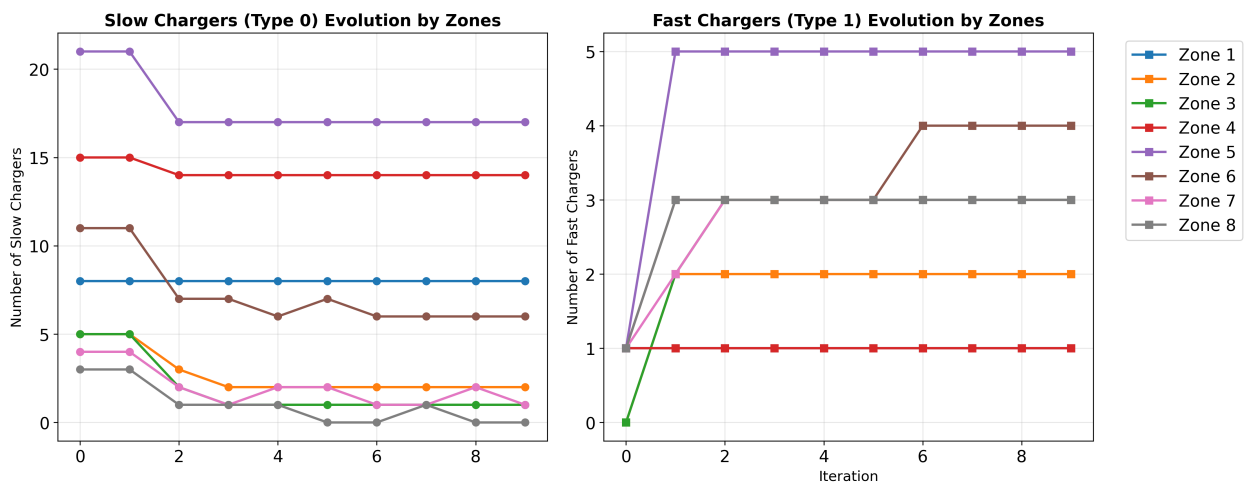


Figure 28 The evolution of the number of slow and fast chargers in each iteration under the setting $\sigma = 2$ and $\gamma = 1$

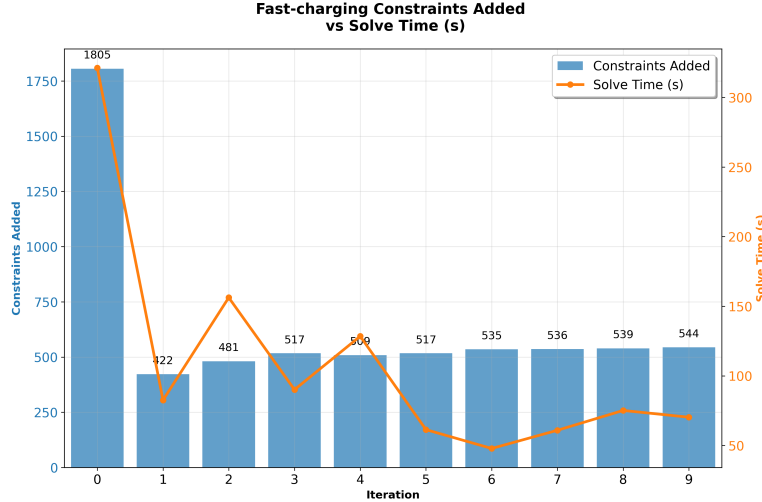


Figure 29 The number of fast-charging constraints incorporated into the scheduling during each iteration and the corresponding solving time for the 39-day instance after applying the constraints with a warm start under the setting of $\sigma = 2$ and $\gamma = 0.5$

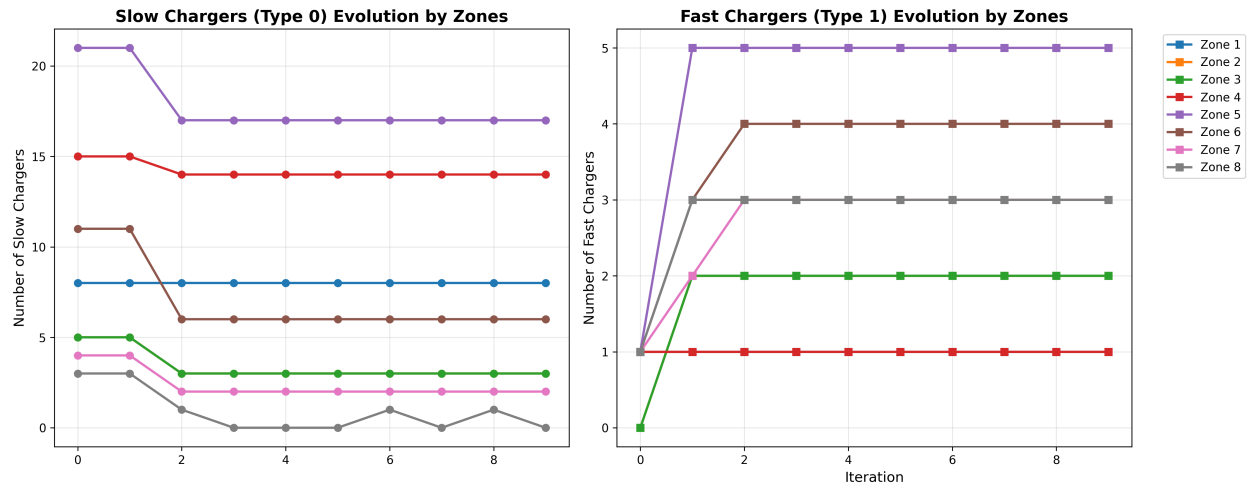


Figure 30 The evolution of the number of slow and fast chargers in each iteration under the setting of $\sigma = 2$ and $\gamma = 0.5$

After obtaining the charger planning results in the final iteration, we post-processed the results by discarding the fast charger results greater than 2, and the rest of fast-charging installation results are taken as hard constraints.